Effects of Intermolecular Interactions and Intramolecular Dynamics on Nuclear Resonance

Cynthia J. Jameson
Department of Chemistry
University of Illinois at Chicago Circle
Chicago, IL, U.S.A.

I. INTRODUCTION

There are several facets to our interest in temperature, solvent, and isotope effects on NMR chemical shifts. Excepting molecular beam studies, the application of NMR to the elucidation of molecular structure and mechanisms of molecular reactions nearly always involves observations of molecules in some environment. Before NMR can be used to obtain structural and mechanistic information unambiguously, the effects of the environment of a molecule on its NMR spectrum must be understood. For example, when a chemical shift is observed in an enzyme-substrate complex for a nucleus in the substrate, the shift can be used to infer structural (e.g., conformational) changes in the substrate induced by the enzyme, but first this requires a separation of the effect due to a change in environment.

At the same time, NMR studies which are necessary to understand and thereby separate out the unavoidable complications due to the effects of the environment may provide fundamental information on the environment itself. This is an equally worthwhile objective, the use of NMR as a probe of intermolecular forces and intramolecular force fields. Thirdly, such studies are intimately connected with the nuclear magnetic shielding function itself, its variation with molecular geometry or intermolecular separation. While closely identified with the NMR technique, nuclear magnetic shielding is a molecular property in the same class as such other properties as electric polarizability and magnetic susceptibility which depend upon the molecular electronic wave functions and are interesting in their own right.

A nuclear resonance signal is a site-specific sensor of intermolecular forces and intramolecular dynamics. As such, it holds the promise of being useful as a unique probe of the intramolecular potential (anharmonic force field) of a single molecule, of the intermolecular potential between two molecules, and of the structure of fluids and solutions. It offers possibilities that are unique in comparison to other physical techniques. One sees only X-A and X-X (not A-A) interactions when using a nucleus in molecule X as a probe, so that it is possible to observe primarily X-A interactions by making the mixture an infinitely dilute solution of X in A. Experimental NMR measurements are capable of extremely high resolution and precision. Furthermore, a great deal of redundancy in information can be obtained so that strong restrictions can be placed on any theoretical interpretation: one can use several nuclei in a colliding pair of molecules as probes, thereby obtaining more information. For example, in studying the collisions between Xe and SiF_4 molecules, the ^{129}Xe, ^{29}Si, and ^{19}F resonances can each be observed. The density and temperature dependence of each of these would have to be satisfied by any theoretical interpretation using one and the same potential function. The ability to use NMR as such a probe depends on our ability to interpret observed shifts in terms of parameters of intra- and intermolecular force fields with the help of theoretical models.

In this review we summarize empirical and theoretical contributions which attempt to describe and explain temperature, solvent, and isotope effects on NMR chemical shifts in two parts: intermolecular effects and intramolecular dynamics. Although observations indicate no unusual behavior with temperature or density upon a change of phase, suggesting that corresponding mechanisms are operative in the liquid phase as in the gas, the state of the theory is not yet sufficiently advanced to deal adequately with condensed phases. Similarly, intramolecular anharmonic force fields are well defined only for the simplest molecules. Thus, this review primarily cites data on fairly simple molecules in the gas phase.

II. INTERMOLECULAR EFFECTS

The nuclear magnetic shielding parameter, σ, which is a measure of the departure of the nuclear environment from a bare nucleus, is determined by the electronic distribution around the nucleus of interest. Since interactions between molecules necessarily affect this distribution to some extent, there are observable effects of intermolecular interactions on the nuclear shielding parameter which can be recorded as frequency shifts of the resonance signal.

A. Observations

Anticipating that the nuclear shielding has a value characteristic of the isolated molecule that is modified by interactions between pairs of molecules and multiple interactions, an appropriate description of the observations in a dilute gas can be given by a virial-type expansion (1)

$$\sigma(T,\varrho) = \sigma_0(T) + \sigma_1(T)\varrho + \sigma_2(T)\varrho^2 + \dots \quad (1)$$

Here, the independent molecule value of the shielding parameter $\sigma_0(T)$ is a function of temperature due to averaging over intramolecular motions,

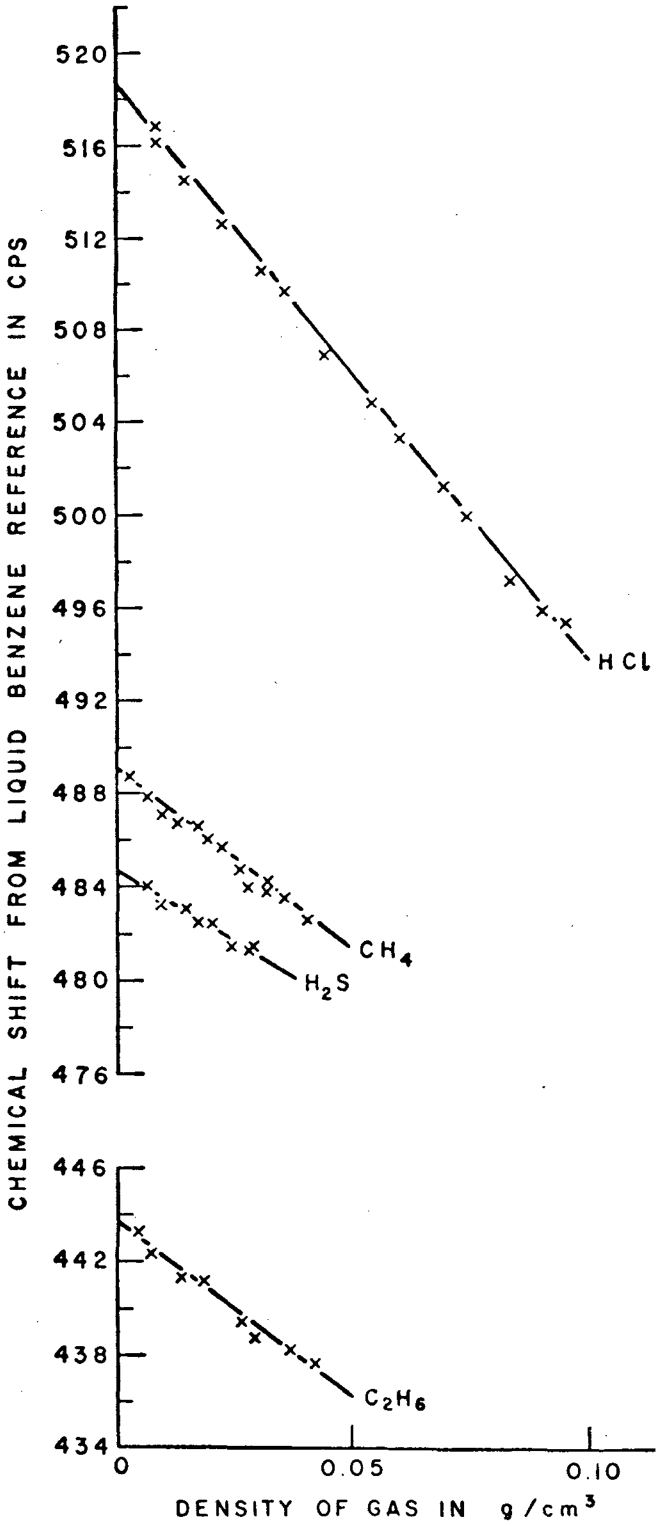

Figure 1. Density dependence of ^1H nuclear resonance in various gases at 30°C and 60 MHz, from Raynes, Buckingham, and Bernstein (2).

and the terms dependent on the density ϱ characterize the intermolecular effects.

By analogy with the second virial coefficient in the usual expansion for PV/RT, $\sigma_1(T)$ may be called a second virial coefficient of the nuclear shielding. In a pure gas X, there is only one $\sigma_1(T)$ observable for each nucleus. In a dilute mixture of gases in which a nucleus in molecule X is observed, there is a $\sigma_1(\mathrm{X,A})\varrho_A$ term for every molecular type A in the mixture, including X itself (2). These $\sigma_1(\mathrm{X,A})$ values depend on the intermolecular potential function for the interaction of an X with an A molecule.

In practice, one thus finds that the resonance frequency of a nucleus in an X molecule in a mixture of gases varies with temperature and with the density of each gas in the mixture. When the observed frequencies at a fixed temperature are plotted as a function of density for moderate densities up to 40 amagat (1 amagat = 2.687×10^{19} molecules/cm^3, the density of an ideal gas at 1 atm and 0°C), the graphs are found to be linear (2-4). Figure 1 shows a typical example of this linear behavior. From such plots, the slope is directly related to σ_1, which can be expressed in units of ppm/amagat.

At very high densities up to 250 amagat, deviations from linear behavior can be expected and were observed in ^{129}Xe in xenon gas (5,6). Figure 2 shows a deviation from linearity well beyond experimental error. Nonlinear behavior with density has also been observed for ^{1}H in C_2H_6 (7), CH_4, and C_2H_4 gases (8).

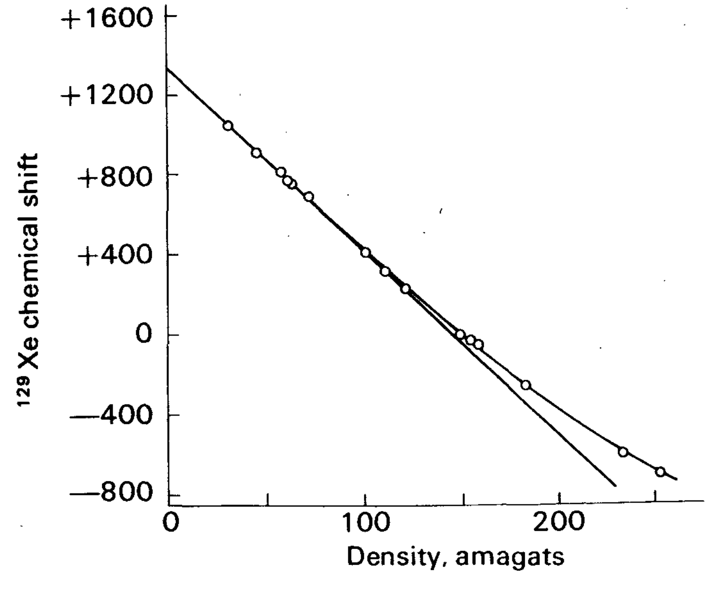

Figure 2. Density dependence of ^{129}Xe resonance in xenon gas at 25°C and 16.6 MHz (6).

Table 1. Pair Interactions Studied by Gas Phase NMR*

Resonant nucleus	Molecules constituting the pair
^{1}H	HCl (also with CH_4, C_2H_6, Kr, CO_2, SF_6, Xe, H_2S, OCS), HBr, C_2H_4, C_2H_6, CH_4 (also with HCl)
^{11}B	BF_3
^{13}C	CO_2 (also with CH_3F, C_2H_4, Kr, Xe), CO, CH_4 (also with Kr, Xe), C_2H_4 (also with CO_2, CH_3F), C_2H_6, CF_4
^{15}N	NNO (also with CF_4, SiF_4, Xe)
^{19}F	CF_4 (also with CH_4, SiF_4, SF_6, Kr, Xe), SF_6 (also with CH_4, CF_4, SiF_4, Kr, Xe), SiF_4 (also with CH_4, CF_4, SF_6, Kr, Xe, PF_5), BF_3, ClF, F_2, CF_3H, CF_3Cl, CF_3Br, CF_3CF_3, CH_3F, NF_3, PF_3, POF_3, PF_5
^{31}P	P_4, PH_3, POF_3, PF_3, PF_5
^{83}Kr	Kr
^{129}Xe	Xe (also with Kr, Ar, CO, N_2, O_2, NO, CO_2, NNO, BF_3, CF_4, CHF_3, CH_2F_2, CH_3F, CH_4, C_2H_2, C_2H_4, C_2H_6, SiF_4, SF_6, HCl, HBr)

*References cited by Rummens (9), Raynes (10), and this review.

These deviations at very high densities are due to the increasing importance of the $\sigma_2\varrho^2 + \sigma_3\varrho^3 + \ldots$ terms which arise from multiple interactions. When measurements are limited to gases of sufficiently low density, linear behavior of frequency with density is always observed. In practice this has been found to hold for densities below 40 amagat.

Operationally, $\sigma_1(T)$ is obtained as

$$\sigma_1(T) = -(1/\nu_0)\lim_{\rho\to 0}(\partial\nu/\partial\varrho)_T \tag{2}$$

The pairs of molecules for which σ_1 has been measured are shown in Table 1. Observed values of σ_1 range from -10^{-3} to about -1 ppm/amagat (9,10). The observed sign of σ_1 is the same for all systems: at a fixed magnetic field, the resonance frequency is uniformly found to increase with increasing density at a given temperature, that is, intermolecular interactions always have a net deshielding effect on the nucleus in a molecule. The range of values of σ_1 not unexpectedly reflects the range in chemical shifts of the nucleus being used as a probe, as shown in Table 2. ^{129}Xe in the xenon atom is found to be an ideal probe of intermolecular interactions (6). ^{129}Xe shifts are very large in comparison to other

Table 2. Range of σ_1 Values for Various Nuclei

	$\mid \sigma_1 \mid$, ppm/amagat
^{1}H	0-0.008
^{11}B	0.0085 in BF_3
^{13}C	0.0022-0.0105
^{15}N	0.0026-0.02
^{19}F	0.006-0.07
^{31}P	0.0023-0.266
^{83}Kr	0.131*
^{129}Xe	0.166-0.75

*In krypton gas, D. Brinkman, *Helv. Phys. Acta* 41, 367 (1968).

resonant nuclei. Being an atom, xenon has no electrical moments and thus no polar interactions with other molecules. Since it has no rotational or vibrational degrees of freedom and no low-lying electronic states, no complications arise from temperature dependence of the shielding in the isolated molecule.

Because the NMR measurements are usually made on samples in cylindrical tubes, a part of the observed σ_1 is due to bulk susceptibility, given to a good approximation by $-2\pi\chi_V/3$, where χ_V is the volume magnetic susceptibility of the substance (11). For light nuclei such as ^{1}H and ^{13}C, this is a sizeable fraction of the observed $\sigma_1(2)$, whereas for heavy nuclei such as ^{129}Xe this is a very small fraction of the observed $\sigma_1(6)$.

Besides the density dependence in gas-phase shifts, gas-to-liquid shifts can also be used as a measure of the effect of like-molecule intermolecular interactions on nuclear shielding. Many of the previously reported gas-to-liquid shifts involved measurements on the gas at one temperature and pressure and on the liquid at another temperature (7). Such comparisons can not properly be considered gas-to-liquid shifts if the temperature coefficient of the shielding is not negligibly small. Ideally, one should observe both the resonance signals in a sample containing a liquid in equilibrium with its vapor at a given temperature (12-14). Since both are then at exactly the same temperature, the intramolecular $\sigma_0(T)$ terms will drop out completely and only the intermolecular interaction effects will be reflected in the frequency shift between the signals. The liquid is always observed at a higher frequency, since intermolecular effects tend to deshield the nucleus, as we have already noted. The ratio of this frequency shift to the density difference between the liquid and vapor gives a very rough measure of σ_1. The measure is only rough because, in principle, higher order terms are expected to be important in the liquid where a molecule "sees" several neighboring molecules at the same time.

For interactions between unlike molecules, the comparable very rough measure of σ_1(X,A) is the shift between the low density gas X and an infinitely dilute solution of X in liquid A (9,15,16). Again, the relative importance of the high order terms in the condensed phase precludes the use of this observable shift for a quantitative measure of σ_1. The shift between the infinitely dilute solution or pure liquid and the zero pressure gas (by extrapolation) at the same temperature gives not just $\sigma_{1\varrho}$ but the total intermolecular contribution to the shielding. Typical magnitudes of gas-to-solution shifts in various non-polar solvents are shown in Table 3. In general, large values of σ_1 measured from the density dependence of gas-phase shifts imply that large solvent shifts can be expected in the condensed phase.

Table 3. Typical Magnitudes of Gas-to-Solution Shifts for a Non-Polar Solute in Various Non-Polar Solvents

Nucleus	*Solute*	*Range of shifts*, ppm	*Reference*
^{1}H	CH_4	−0.225 to 0.781	32
^{13}C	CH_4	5.3 to 12.1	32
^{19}F	CF_4	3.04 to 7.90	9
^{31}P	P_4	21.1 to 93.0	*

*G. Heckmann and E. Fluck, *Z. Naturforsch.* **24b**, 1092 (1969), **26b**, 63 (1971).

The observed temperature dependence of σ_1 values has been generally in the direction of decreasing absolute value of σ_1 with increasing temperature (5,13,17-21). Although in some cases an apparent minimum may have been observed in the $\sigma_1(T)$ function of some nuclei, the existence of the minimum is not yet unequivocally established within the relative precision of the temperature dependence (14). For ^{129}Xe, the temperature dependence of σ_1 is large, and since the shifts are very large, the relative precision of the data is high. In these cases, the $\sigma_1(T)$ functions are reasonably well defined (18-22). An unusual temperature dependence, increasing magnitude of σ_1 with increasing temperature, has been observed in two such cases (22). Some examples of $\sigma_1(T)$ for ^{129}Xe are shown in Figure 3. A comparison of the $\sigma_1(T)$ functions for various nuclei in selected molecular pairs is shown in Figure 4.

Some general empirical observations about σ_1 are the following: (1) The sign of σ_1 is negative, that is,

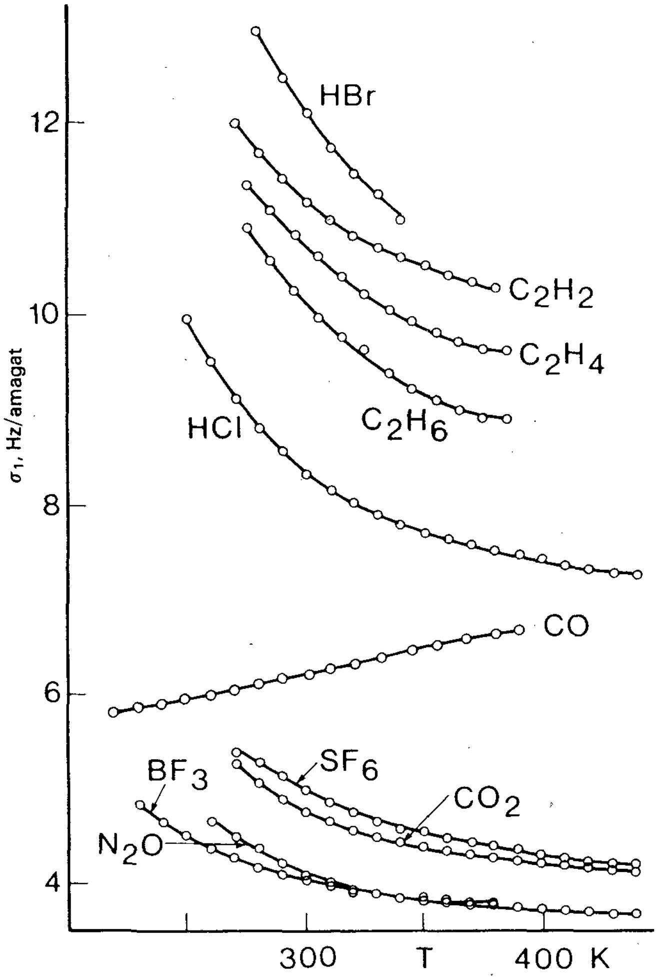

Figure 3. Temperature dependence of σ_1(Xe,A), the effect of intermolecular interactions on ^{129}Xe nuclear magnetic shielding in various gases A, at 24.897 MHz. Positive slope of curve for A = CO is one of two unusual cases.

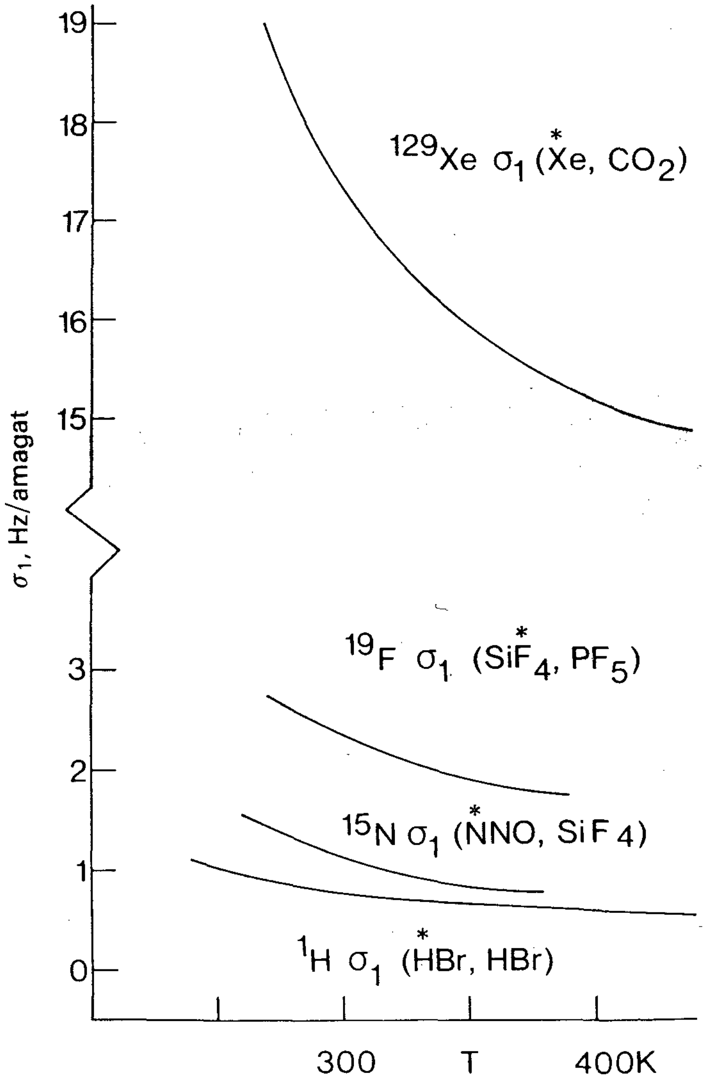

Figure 4. $\sigma_1(T)$ for various nuclear species at 90.0 MHz. Compare scale of σ_1(Xe,CO$_2$) curve here with that in Fig. 3.

one always observes a downfield shift with increasing density. (2) Systems with large values of σ_1 tend to have a large change in σ_1 with temperature. (3) In the usual temperature dependence of σ_1, the magnitude of σ_1 decreases with increasing temperature, although at least two unequivocal exceptions are known. (4) The magnitude of σ_1 depends on the atomic number just as the range of chemical shifts does. (5) More centrally located nuclei tend to have smaller σ_1 values. As a consequence of these trends, the shift of the liquid and gas resonance signals with temperature may be quite different, since gases are generally observed at constant volume and liquids at constant pressure. The shift of the liquid signal with temperature is usually dominated by the temperature coefficient of its density, which is generally negative. Thus, with increasing temperature, one would observe an upfield shift in the liquid and in many cases (see section III) a downfield shift in the gas.

B. Models for Intermolecular Effects on Nuclear Shielding

Non-specific solvent effects in NMR have been interpreted in terms of two types of models. On the one hand, the solvent is considered as a continuum and the observed shifts are correlated with some bulk property such as dielectric constant or refractive index. On the other hand, the shift is interpreted in terms of the interaction between a pair of molecules.

1. Continuum Models

Continuum models were specifically designed to apply to gas-to-liquid and gas-to-solution shifts. While a continuum model may seem questionable, it has an indisputable advantage: one does not have to worry about higher order collisions or the validity of considering pairwise interactions in a condensed phase. Another advantage is its dependence on parameters characteristic of bulk samples, which are readily obtainable.

Several continuum models have been proposed. We will consider in particular those of Linder (23) and de Montgolfier (24). These models are based on the Onsager continuum model whch has met considerable success in the theory of dielectrics, such as the calculation of dipole moments from dielectric constants (25). The permanent dipoles in a continuum in the Onsager model are replaced with spontaneous oscillating dipoles in a non-polar solvent. In the continuum models, one solute molecule is singled out and treated as though the surrounding molecules are replaced by a uniform dielectric medium. The non-polar solute molecule with its spontaneous oscillating moment, when brought into the cavity, polarizes the continuum, which in turn creates a reaction field at the solute. The oscillating moment and the reaction field reach equilibrium average values which are then used to calculate the dispersion energy and $\overline{F^2}$, the mean square field. In the case of polar solute molecules, the solute is represented by a point dipole at the center of a spherical cavity and the solvent by a continuum of static dielectric constant. Here, a linear electric field as well as quadratic field effects are important in addition to the $\overline{F^2}$. The basic difference between de Montgolfier's and Linder's theories is that the former considers the electrical anisotropy of chemical bonds. As a result of this, the reaction field is not constant over the cavity as it is in Linder's theory.

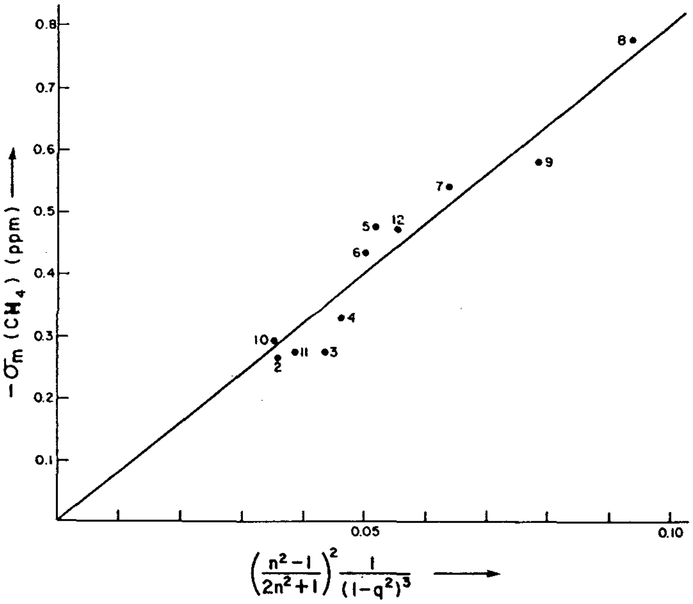

Figure 5. *Proton gas-to-liquid shifts of CH_4 at 298 K, corrected for bulk susceptibility, plotted against continuum-model function f(n,q) for solvents ranging from CH_2I_2 (8) to CS_2 (9) to $C_6H_5NO_2$ (19), from F. Mourits (32). This function is for de Montgolfier's model, modified by F.H.A. Rummens, *J. Chim. Phys.* **72**, 448 (1975), where *n* is the refractive index and *q* is the ratio of the distance between the resonant nucleus and the center of mass of the solute to the sum of the molecular radii of solute and solvent.

The continuum models have been tested extensively. Homer (26) and Rummens (9) give comprehensive reviews and comparative analyses of these continuum theories and their subsequent modifications. Typically, a given nucleus in a given solute molecule in a series of related solvents has NMR shifts that show a linear correlation with that function of refractive index characteristic of the model (see Figure 5). Although continuum theories have been useful in the systematic classification of some solvent effects on NMR shifts, they appear to be inadequate in the following ways. For one solute with various solvents, one finds approximately linear correlations, but these exhibit a distinctly non-zero intercept which can not be rationalized. Large deviations appear when other solvents are included, especially those with disparate dielectric constants. Even for solutes very similar in chemical nature, rather different proportionality constants are apparently required. Differences are also observed when different nuclei on the same solute molecule are compared. It therefore seems that none of the continuum models has general applicability in the interpretation of gas-to-liquid or gas-to-infinitely-dilute-solution shifts.

There are several factors which may be responsible for the lack of success of continuum models, especially for non-polar solvents. The very concept of a cavity in a continuous medium is not realistic for van der Waals effects since one is dealing with an R^{-6} dependence with van der Waals forces (rather than the R^{-3} dependence of dipolar fields) which restricts the interaction to the molecules in the immediate vicinity of the solute rather than to the bulk of the solvent. Moreover, these theories ignore the detailed shape of the solute molecules. Another major difficulty lies in the assumption that the orientation of the solvent molecules, with respect to each other and to the solute, is completely random. The effect of directionally dependent molecular interactions has been considered by Buckingham *et al* (27). However, until details of the structures of liquid mixtures are incorporated into the theory, it is unlikely that continuum and other types of theoretical approaches will prove adequate for a unified interpretation of solvent shifts. The most obvious failure of continuum models is that they predict zero temperature dependence if the volume is kept constant, as is the case with gas-phase studies. In other words, they predict no temperature dependence in σ_1.

2. Pair Interaction Models

Pair-interaction models have been applied not only to the density dependence of gas-phase shifts but also, with considerably less justification, to gas-to-liquid or gas-to-solution shifts (9). From a phenomenological point of view, the virial-type expansion used for a dilute gas is a convenient starting point. In $\sigma(T,\varrho) = \sigma_0(T)\varrho + \sigma_1(T)\varrho + \sigma_2(T)\varrho^2 + \ldots$, the $\sigma_1(T)$ function for a spherically symmetric solute molecule and a spherically symmetric solvent molecule can be written as (28)

$$\sigma_1(T) = 4\pi\int_0^\infty \sigma(R)\exp[-V(R)/kT]R^2dR \tag{3}$$

where R is the intermolecular separation. $\sigma(R)$ is a shielding function, characteristic of the nucleus observed and of the interacting pair of molecules, which vanishes at infinite separation. Approaching the limit of zero density in obtaining $\sigma_1(T)$ experimentally is consistent with the use of the virial expansion and the pair-interaction model. However, extension of this model to the interpretation of gas-to-liquid or gas-to-solution shifts can be expected to lead to difficulties. The observation of nonlinear behavior of medium shifts with density, from low density gas through the liquid range in some systems, indicates non-negligible higher-order contributions in the liquid (9).

In pair-interaction models, the model supplies the form of $\sigma(R)$. This function may be the result of a quantum mechanical calculation of nuclear shielding in a molecular pair at various intermolecular separations. There are not many available functions of this type at this time. Molecular systems which have received some attention are H_2-He, CO-He, CH_4-He, and CH_4-CH_4 (29-31). Although the results are promising, wide application to other molecular systems is not yet forthcoming.

A general form of $\sigma(R)$ has been introduced by Raynes *et al* (2). σ_1 is considered as a sum of separable contributions

$$\sigma_1 = \sigma_{1b} + \sigma_{1w} + \sigma_{1E} + \sigma_{1a} + \sigma_{1rep} \tag{4}$$

which are, respectively, the bulk susceptibility term, the van der Waals term, the electrical terms for solutes with non-vanishing electrical moments, the magnetic anisotropy term for solutes with non-spherical structure, and the short range or repulsive term. In the earliest form of the Raynes-Buckingham-Bernstein (RBB) theory (2), the van der Waals term in $\sigma(R)$ was taken to be of the form $-3B\alpha_2 I_2 R^{-6}$, in which the polarizability and ionization potential of the solvent molecule affect the shielding function, and an empirical constant B is supposed to be characteristic of the solute molecule. Later refinements involve the polarizability of the solute as well, for example, $-3B\alpha_2 I_2[I_1/2(I_2 + I_1)]R^{-6}$ (32).

The empirical parameter B is taken to be the same one which appears in the electrical terms, $-A\overline{E}_{||}$ $-B\overline{E^2}$, reflecting the contribution to the nuclear shielding induced by electric fields arising from a neighboring solvent molecule that possesses polar groups or is polarized by a polar solute. The electrical terms for a nucleus in a polar molecule interacting with a polar molecule include dipole-dipole, dipole-induced-dipole, and dipole-quadrupole interactions. For a nucleus in a polar molecule interacting with a non-polar molecule, the contributions are due to dipole-induced-dipole and dipole-quadrupole interactions. For a nucleus in a non-polar molecule interacting with a polar molecule, the electrical contributions are neglected. Physically, the parameter A is associated with the ease with which charge may be displaced along the bond connecting the resonant nucleus (28,33). The B parameter on the other hand is an average over more than one coefficient, say $B_\perp$ and $B_{||}$, for a nucleus in an axially symmetric bond. These parameters are expected to be related to the analogous A and B parameters associated with the change in nuclear shielding in an isolated molecule in the presence of the static uniform electric field (34-37). However, the latter should only be considered a first approximation to the shielding changes due to intermolecular electric fields, since the fields due to polar molecules can be shown to be highly non-uniform (36,38). A better description of the non-uniform nature of the electric fields of polar groups can be obtained by expressing the shielding as an expansion in terms of the field and its derivatives, the first of which is the linear field gradient. The effects of an electric field gradient on nuclear magnetic shielding are not necessarily small (38,39).

The magnetic anisotropy term is considered important for a solvent molecule which exhibits anisotropy in its molecular magnetic susceptibility and has a preferred relative orientation with respect to the solute (27,28). Buckingham *et al* (27) have shown that chemical shifts arise in liquid solutions due to the anisotropy in the susceptibility of solvent molecules. The contribution to the nuclear magnetic shielding due to the anisotropy of the susceptibility of axially symmetric molecules is

$$\sigma_a = -(\chi_{||} - \chi_{\perp})\,(3\cos^2\theta - 1)/3R^3 \tag{5}$$

where θ is the angle between R and the symmetry axis of the solvent molecule, and $\chi_{||}$ and $\chi_{\perp}$ are the solvent magnetic susceptibilities parallel and perpendicular to the symmetry axis. For a model of a liquid made of hard-sphere solute and hard-cylinder solvent molecules, $<\sigma_a> \simeq (\chi_{||} - \chi_{\perp})/3R^3$, since the mean value of $(3\cos^2\theta - 1)$ is about -1. On the other hand, the effect of a disk-shaped solvent molecule such as benzene on the nuclear shielding of a spherical molecule such as Xe would be $<\sigma_a> \simeq -2(\chi_{||} - \chi_{\perp})/3R^3$ since in this case the mean value of $(3\cos^2\theta - 1)$ is about 2. For liquid solutions, $|<\sigma_a>|$ is of the order of 0.5–1 ppm (40).

If this asymptotic form of the anisotropic long range contribution is added to $\sigma(R)$ in gases, there should be a non-zero contribution to σ_1 from this term when the intermolecular potential is a function of orientation as well as distance. There will be a sizeable σ_{1a} contribution if (a) $\chi_{||} - \chi_{\perp}$ is large, and (b) if the average $<3\cos^2\theta - 1>$ is large. For example, for a pair of molecules like Ar and HCl, the attractive and repulsive parts of $V(R,\theta)$ are each taken to be of the form $V(R)\,[1 + a_1\cos\theta + a_2(3\cos^2\theta - 1)]$ where $V(R)$ is the isotropic part (41). The average value $<3\cos^2\theta - 1>$ is large if a_2, the coefficient of the $3\cos^2\theta - 1$ term in the attractive part of $V(R,\theta)$, is large. For two non-polar molecules, such as Xe and CO_2, this coefficient is estimated by $(\alpha_{||} - \alpha_{\perp})3\alpha_{Xe}$.

Values of the anisotropy of the polarizability of molecules of a gas are available from measurements of depolarization of light scattered by the gas (42). The values of $\chi_{||} - \chi_{\perp}$ can be obtained by observing Zeeman molecular effects under high resolution (43,44). The temperature dependence of the long range anisotropic term is different from that of the isotropic term. While the isotropic part of σ_1 has a non-zero limiting value at infinite temperature, the anisotropic term has a limiting value of zero and becomes more important at low temperatures. Thus, we expect a more pronounced temperature dependence (a steeper curve at low temperatures) if the isotropic and anisotropic parts have the same sign, and a less pronounced temperature dependence if their signs are opposite. It was found that while Xe-BF_3 and Xe-NNO have nearly the same values at temperatures above 300 K, they deviate from each other at lower temperatures, the Xe-NNO having a somewhat steeper curve (see Figure 3) than the Xe-BF_3 (21). This is what would be expected from the anisotropy of the interaction with Xe of a rod-shaped molecule like NNO as opposed to a disk-shaped molecule like BF_3.

The repulsive or short-range contribution to $\sigma(R)$, which is not conceptually separable from the long-range contributions considered above, is not so clearly defined. For non-polar molecules it could be identified with the $\sigma(R)$ one might obtain from a quantum mechanical calculation of nuclear magnetic shielding in a molecular pair, using uncorrelated wavefunctions (29-31). This term is neglected in most applications of the model or is presumed to approximately cancel out the higher dispersion (other than R^{-6}) terms which are likewise neglected. There is some evidence that this may be justified for protons (45). For a pair of xenon atoms, Adrian has proposed that the short-range contributions account for practically all of the ^{129}Xe σ_1 (46). However, the temperature dependence of his calculated $\sigma_1(T)$ does not agree with experiment (47).

An additional factor, called the site effect, has been considered in comparing σ_1 for various nuclei in the same solute molecule. The site effect was put into quantitative form by Rummens and Bernstein (48). The use of the solute-nucleus to solvent-center distance rather than the solute-center to solvent-center distance as a more appropriate R was expected to improve correlations between solutes in gas-to-solution shifts and to lead to a better transferability of the B parameters between solute-solvent combinations. The best test of the site factor was provided by Rummens *et al* (49) using the proton shifts from gas to solutions in binary systems made up of $X(CH_3)_4$ molecules (X = C, Si, Ge, Sn, Pb) chosen for their lack of dipole moments and for their nearly spherical shapes (thus σ_{1E} and σ_{1a} are probably negligible). In the same paper, the gas-to-solution shifts of the CH_3 and the CH_2 protons in $Si\,(CH_2CH_3)_4$ in six isotropic non-polar solvents were found to differ by 0.03 to 0.05 ppm, with the shifts for the CH_3 being greater than for CH_2, as predicted by the site-factor model. In general, peripheral nuclei tend to have larger σ_1 values than more centrally located nuclei. For example, the end ^{15}N in NNO was found to exhibit a σ_1 2.8 to 3.5 times as large as the central ^{15}N, depending on the temperature (14). However, this generally observed trend need not be entirely due to the site factor.

Although it has been applied to shifts in condensed phases, the pair-interaction model applies strictly only to the dilute-gas phase. Here, the pair interaction model was moderately successful in interpreting ^{1}H (2,4) and ^{19}F shifts (50). However, as more data were collected, the model deviated from experiment in terms of constancy of the empirical parameters, agreement with data within experimental accuracy, and also in the implicit temperature dependence (6,17). Since the entire temperature dependence of σ_1 is in the $\exp[-V(R,\theta,\phi)/kT]$ and not in the $\sigma(R,\theta,\phi)$ function, the model empirical parameters A and B ought to be temperature independent. Data taken over a range of temperatures cannot be fitted with the same set of A and B parameters. While part of this discrepancy must be due to the quality of some of the intermolecular functions $V(R,\theta,\phi)$ which were used, a substantial part of the discrepancy may also be due to the simplifications used in implementing the model. However, this is not sufficient reason to reject the partitioning of the observed σ_1 into the respective contributions. The omission of a method for estimating or calculating the short-range contributions may be the method's only substantial weakness. As more calculations of short-range $\sigma(R)$ become available, some general method of quantitative estimation of the short-range contributions may become apparent.

3. The Intermolecular Shielding Function, σ(R)

NMR is potentially a very useful probe of the intermolecular potential function. The high precision (1 part in 10^8 or 10^9) and the redundancy of information offered by the use of several resonant nuclei in the interacting pair make it an attractive molecular quantity for the determination of intermolecular forces. By studying systems for which the intermolecular potential functions are known to a greater extent than for others, we hope to determine the nuclear shielding as a function of internuclear separation and configuration (47). Only when the $\sigma(R)$ function is satisfactorily characterized in a general way by a combination of experiment and theoretical calculations, will the determination of intermolecular potentials from NMR experiments become possible. At the present time, less is known about the form of $\sigma(R,\theta,\phi)$ than about $V(R,\theta,\phi)$.

The chemical shielding function $\sigma(R)$ for two interacting Xe atoms has been empirically obtained by mathematical inversion of σ_1 data for xenon (57) from equation (3), using the most accurate Xe-Xe potential function available, that of Barker *et al* (51). The empirical $\sigma(R)$ which was obtained appears to have a shape not unlike that of the incremental polarizability of interacting rare gas atoms, $\alpha(R)$, except for the sign. $\sigma(R)$ for a pair of Xe atoms is positive at small R, has a node in the vicinity of R_0, a minimum in the vicinity of R_e and approaches zero as R goes to infinity. It was found that a fair fit to the experimental $\sigma_1(T)$ is obtained from a $\sigma(R)$ function of the form $V^2(R)$, which mimics the behavior of the empirical shielding function in the intermolecular distances most significant in determining $\sigma_1(T)$ (47).

The non-monotonic dependence of $\sigma(R)$ on intermolecular distance was surprising at first. However, upon comparison with other systems it appears to be quite reasonable. For example, for two interacting F atoms, the nuclear shielding relative to the bare F nucleus at three limiting cases are:

$\sigma_0 = +470.71 \times 10^{-6}$ for an isolated F atom (52)

$\sigma_0 = -232.6 \times 10^{-6}$ for the F_2 molecule at $R = 1.418$ Å (53)

$\sigma_0 = +1237.64 \times 10^{-6}$ for the united argon atom (52)

Thus, relative to the isolated F atoms, the shielding function $\sigma(R)$ has the following values: 0 at $R = \infty$, -703×10^{-6} at R=1.418 Å, and $+766.93 \times 10^{-6}$ at R=0.

Hence, for two interacting F atoms the shielding function is non-monotonic and has at least one node between $R = 1.418$ Å and $R = 0$. It is therefore not surprising that the empirical $\sigma(R)$ which was obtained for two interacting Xe atoms appears to have non-monotonic dependence on internuclear distance. Theoretical calculations of the short range part of $\sigma(R)$ for ^{1}H in CH_4 interacting with He or CH_4 also reveal a non-monotonic function (31).

III. INTRAMOLECULAR DYNAMICS

The effects of intramolecular dynamics (vibration and rotation) on nuclear shielding were theoretically predicted by Ramsey (54) and have been observed in two ways. First, there is an observable temperature dependence of the resonance frequency (apart from that due to the temperature dependence of the liquid reference) in the limit of zero pressure. Second, there is an observable shift upon isotopic substitution of neighboring nuclei. The first is a measure of the change with temperature of the thermal average of Δr (mean displacement), $\langle(\Delta r)^2\rangle$ (mean square displacement), etc., whereas the second reflects the difference in $\langle\Delta r\rangle$, $\langle\Delta\alpha\rangle$, $\langle(\Delta r)^2\rangle$, etc. between the heavier and lighter isotopic forms (isotopomers). Both are effects of differences in averaging over nuclear configuration as the molecule undergoes vibration and rotation.

A. Observed Temperature Dependence of Nuclear Resonance in Isolated Molecules

In the virial expansion of nuclear shielding in a pure dilute gas, $\sigma(\varrho, T) = \sigma_0(T) + \sigma_1(T)\varrho + \ldots$, only the effects of the intermolecular interactions give rise to the density dependence. Since both the density dependence and the temperature dependence of the resonance signal of the NMR-sensitive nucleus may be measured by observing samples of varying low densities over a suitable temperature range, both $\sigma_0(T)$ and $\sigma_1(T)$ can be obtained separately. From the temperature dependence of the sample in the limit of zero pressure, we can infer $d\sigma_0(T)/dT$ although it is not possible to measure the absolute value of σ_0 itself. This means that we can measure the $\sigma_0(T)$ function, the temperature dependent nuclear shielding in the isolated molecule, except for an additive constant.

A part of the temperature dependence observed in the limit of zero density is the temperature dependence of the liquid substance used to stabilize the magnetic field via a field-frequency internal lock. Since the liquid reference is at the same temperature and magnetic field as the sample (in practice the sealed sample tube of gas is in an NMR tube with some liquid reference in the annular region), the applied magnetic field is varying to the extent that the resonance frequency of the reference is temperature dependent. Thus, $d\nu_{ref}/dT$ has to be measured independently and subtracted out (55). When the reference temperature dependence and the density-dependent contributions are removed, only the resonance frequency change characteristic of an independent molecule remains. Figure 6 shows examples.

A convenient way of expressing the intrinsic temperature dependence of the isolated molecule shown in Figure 6 is in terms of a difference, $\sigma_0(T) - \sigma_0(300\text{ K})$, where 300 K is arbitrarily chosen as a standard temperature. This difference function has been measured for ^{19}F, ^{15}N, ^{11}B, ^{13}C, ^{31}P, and ^{1}H nuclei in various small molecules (14,56-65). Figures 7 and 8 present some of the results.

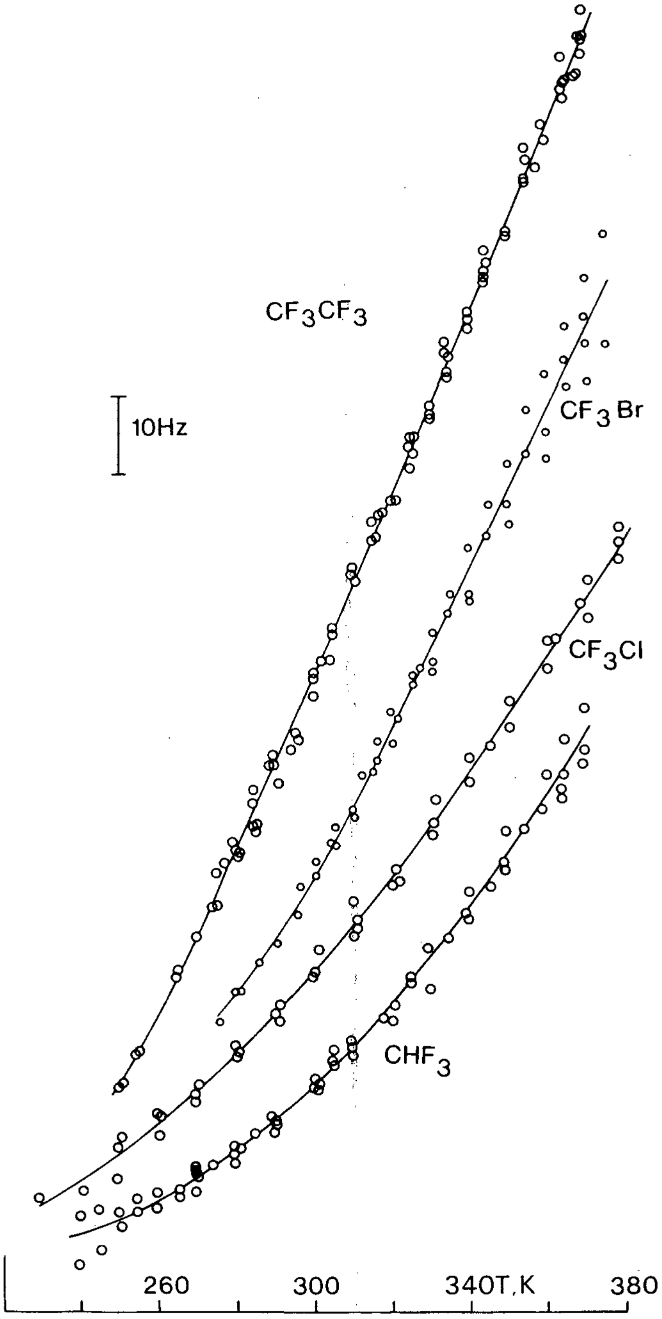

Figure 6. Temperature dependence of ^{19}F resonance frequency at the limit of zero density in various molecules at 84.7 MHz (63).

In general, it is found that deshielding occurs with increasing temperature. The temperature dependence of centrally located nuclei such as ^{11}B in BF$_3$, ^{13}C in CH$_4$ and ^{31}P in PF$_5$, have been found to be generally smaller (both $d\sigma_0/dT$ and $d\sigma_1/dT$ are small) than that of peripheral nuclei (61,65). This is most apparent in the NNO molecule in which both the end and central ^{15}N nitrogen were observed (14). We see in Figure 8 that the end ^{15}N has a greater temperature dependence in the isolated molecule. Of the functions shown in Figures 7 and 8, the best defined $\sigma_0(T)$ are those of ^{19}F in which the relative error measured as a percentage of the total observed shift varies

Continued on page 15

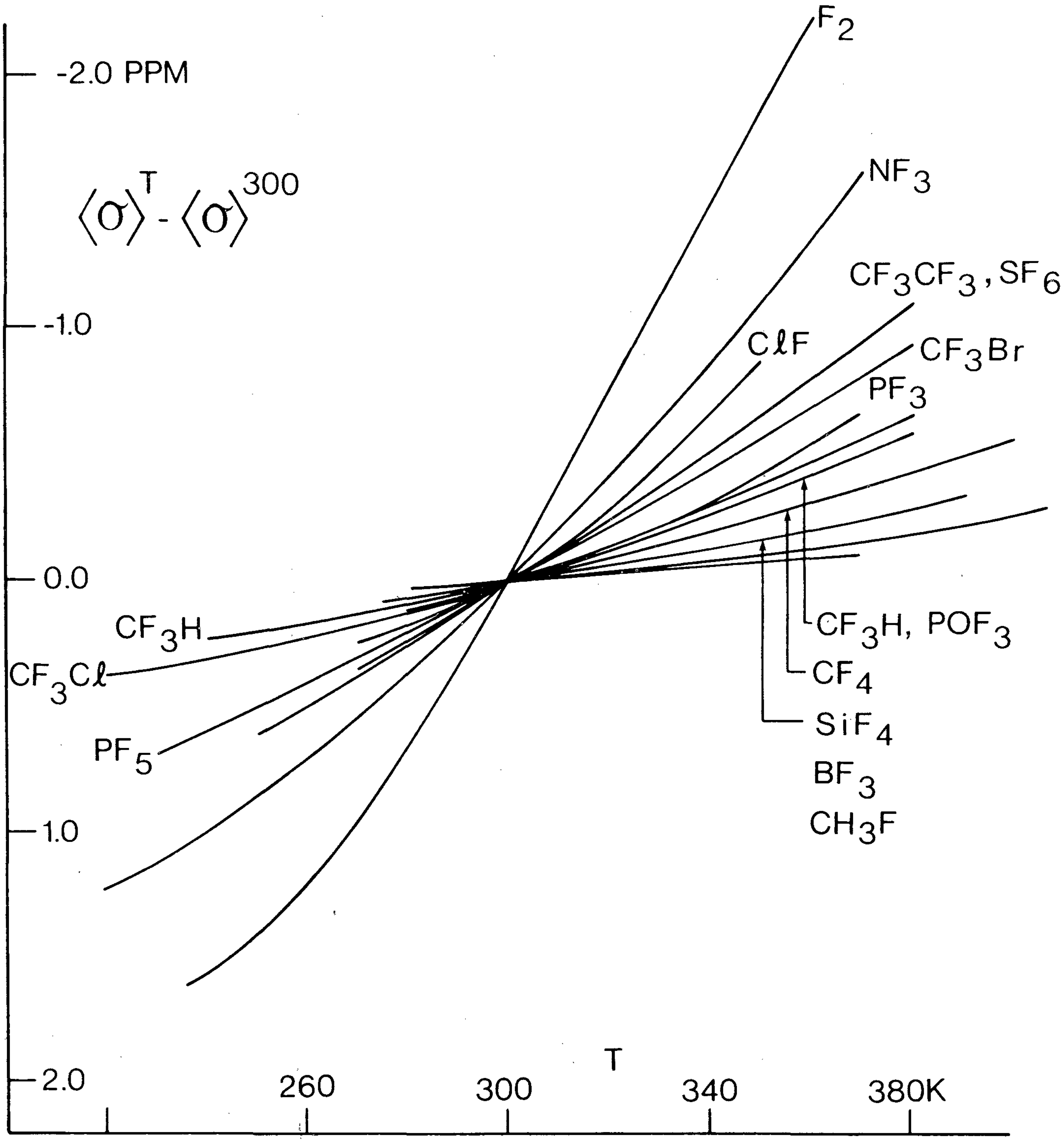

Figure 7. Experimental shielding difference functions for ^{19}F nucleus in various isolated molecules (65).

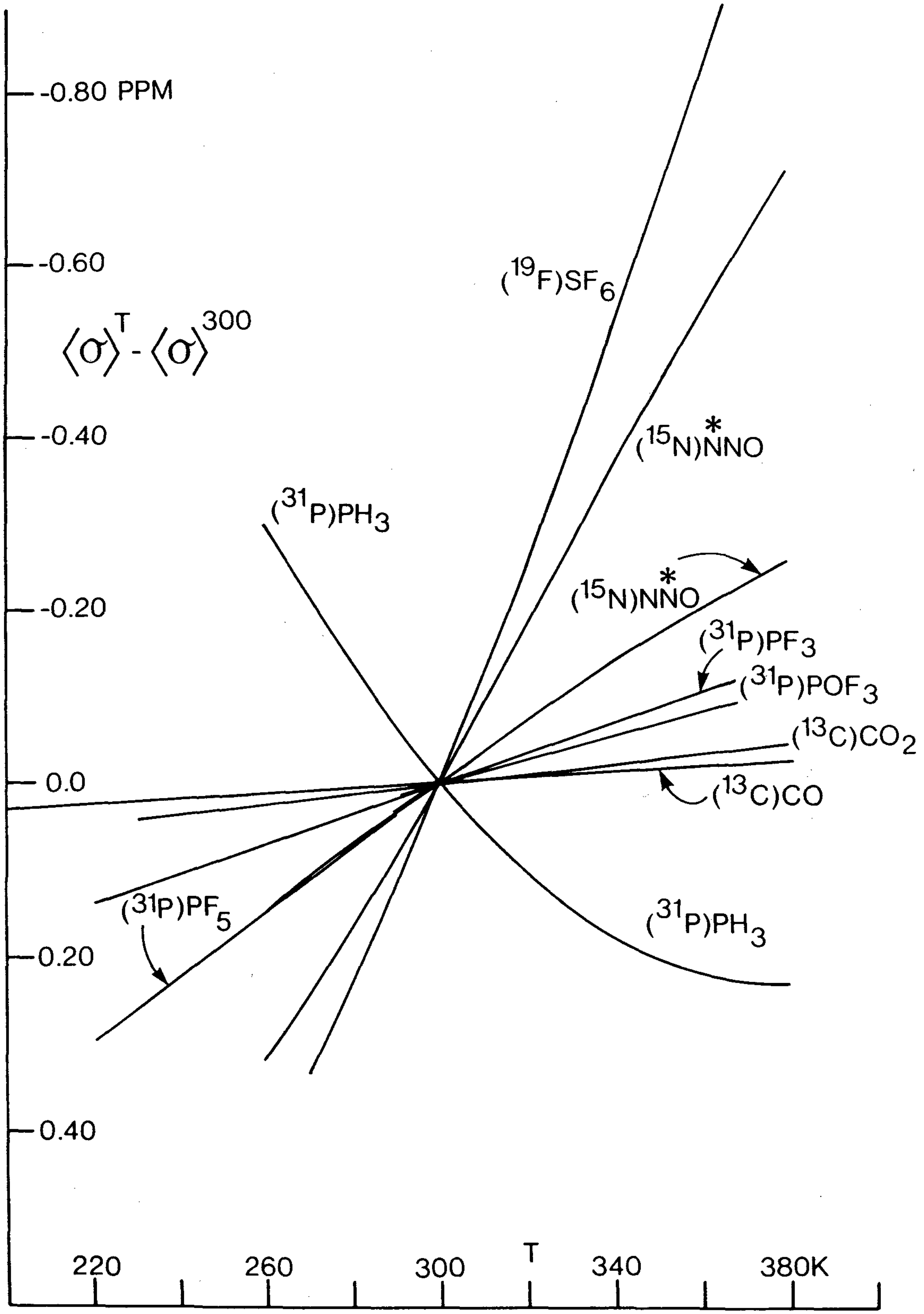

Figure 8. Experimental difference functions for various nuclei shielding (65). Several ^{19}F functions are included for comparison.

from 0.5 to 2.5%. ^1H shifts are so small that $\sigma_0(T)$ functions can not be reliably obtained. There is a large uncertainty associated with the reported $\sigma_0(T)$ of ^1H in HCl and HBr (56,57). ^{11}B in BF_3 and ^{13}C in CH_4 show no measureable $d\sigma_0/dT$ (61).

B. Vibrational and Rotational Effects on Nuclear Resonance

The nuclear shielding in an "isolated molecule" is actually observed as the nuclear shielding in the limit of pressure approaching zero. Yet, the pressure must be high enough so that collisional interactions cause a given molecule to pass through a representative number of thermally accessible vibrational states in a time which is short compared to the reciprocal of the NMR frequency difference between nuclei in different vibrational states. Thus, mathematically speaking, one does not extrapolate the results to a true zero pressure, but to a pressure which is so low that collisional deformation of the molecules no longer contributes to σ, while there are still enough collisions to provide the required rate to transitions between vibrational and rotational states.

The observed isotropic nuclear shielding of a nucleus in an isolated molecule is a statistical average of the nuclear magnetic shielding tensor over all possible orientations of the molecule in the magnetic field. It is also an average over all possible rovibronic states of the molecule, weighted according to the fraction of molecules occupying that state at that temperature. Thus, the value of the resonance frequency of a nucleus in a gas sample extrapolated to zero density at a given temperature is a weighted average of the values characteristic of each occupied state.

Alternatively, the chemical shielding can be considered as a function of the nuclear configuration of the molecule. The internuclear distances in a molecule are affected by the vibrational and rotational motions of the molecule. Since the vibration is in general anharmonic, the vibrating molecule is more or less deformed from the equilibrium configuration. In addition, the centrifugal forces due to the overall rotation act on the component atoms to shift their average positions away from the center of gravity of the molecule. The observed nuclear shielding is therefore a value characteristic of the thermal average of internuclear distances.

For a diatomic molecule, the effects of anharmonic vibration and centrifugal distortion are that the mean bond length increases with increasing temperature (66). As the vibrational quantum number increases, the average internuclear distance R increases because of the anharmonicity (Figure 9). As the rotational quantum number increases, the mean value of R increases because the molecule is not completely rigid. Thus, both anharmonic vibration and centrifugal distortion cause R to increase with increasing temperature. Harmonic vibrational contributions also appear, at second-order (66). Since the nuclear shielding in a diatomic molecule varies with R, a temperature dependence of the nuclear shielding will be observed.

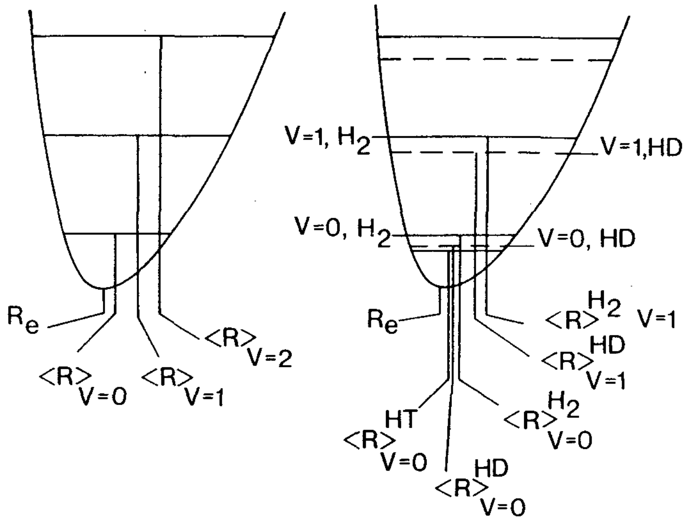

Figure 9. Effect of anharmonicity on average internuclear separation in a diatomic molecule. Diagrams are not drawn to scale so that the shape of the potential and differences between isotopically related molecules are exaggerated to emphasize the effect. Vibrational frequencies of H_2, HD, and HT are 4395.2, 3817.09, and 3608.3 cm^{-1}, respectively.

A dependence of nuclear shielding on isotopic masses of neighboring nuclei due to anharmonic vibration and centrifugal distortion can also be expected. While the potential-energy curves for H_2 and HD are virtually identical (this is the basis of the Born-Oppenheimer approximation), the vibrational levels of the heavier isotopomer sit lower in the potential curve (Figure 9). For corresponding vibrational quantum numbers the mean value of R is smaller for the heavier molecule. As a molecule rotates, all atoms tend to move away from the center of mass, but the centrifugal distortion in the molecule with the lighter atoms is greater than in the corresponding isotopomer. Thus, both anharmonic vibration and centrifugal distortion contribute to a larger mean bond extension in the lighter isotopomer than in the heavier one. Since nuclear shielding in a diatomic molecule varies with internuclear separation, an isotope effect in the nuclear shielding will be observed.

The above arguments are easily expressed in quantitative terms for a diatomic molecule which has only one internal coordinate. To deal quantitatively with a general polyatomic molecule, we have to consider a complete non-redundant set of coordinates such as normal coordinates.

1. The Average Nuclear Shielding in Powers of the Normal Coordinates

Provided that the Born-Oppenheimer approximation is valid, any molecular electronic property such as nuclear magnetic shielding can be expanded in terms of powers of the dimensionless normal coordinates of the molecule

$$\sigma = \sigma_e + \sum_i (\partial\sigma/\partial q_i)\, q_i + \tfrac{1}{2}\sum_{i,j}(\partial^2\sigma/\partial q_i \partial q_j)\, q_i q_j + \ldots \quad (6)$$

The average of nuclear shielding over a given vibrational state, $\langle\sigma\rangle_v$, would then be in terms of vibrational averages of dimensionless normal coordinates $\langle q_i\rangle_v$, $\langle q_i q_j\rangle_v$ and the thermal average, $\langle\sigma\rangle^T$, would be in terms of thermal averages of these normal coordinates $\langle q_i\rangle^T$, $\langle q_i q_j\rangle^T, \ldots$. These averages of the normal coordinates are calculated from perturbation theory of vibration-rotation or from the use of contact transformations (67). The expectation values $\langle q_i\rangle$ vanish for all but the totally symmetric vibrational modes. They also vanish for a rigid rotor-harmonic oscillator. For a totally symmetric coordinate q_s

$$\langle q_s\rangle_v = -[3k_{sss}(v_s + \tfrac{1}{2}) + {\sum_{s'}}' k_{ss's'}(v_{s'} + g_s/2)\,]/\omega_s + \langle q_s\rangle_v^{cent} \quad (7)$$

where the molecular constants q_s and ω_s are the degeneracy and the harmonic frequency of the sth vibrational mode, and the cubic force constants $k_{ss's'}$ are the coefficients of the coordinates $q_s q_{ss'}{}^2$ in the expansion of the intramolecular potential function. Equation (7) includes the contributions from anharmonic vibration and centrifugal distortion (the last term).

The thermal average of $(v + \tfrac{1}{2})$ over discrete vibrational levels is

$$\langle v + \tfrac{1}{2}\rangle^T = \tfrac{1}{2} + \frac{e^{-hc\omega/kT}}{1 - e^{-hc\omega/kT}} = \tfrac{1}{2}\coth(hc\omega/2kT)$$

For the centrifugal distortion, a classical average (an integral) over rotational states rather than a sum over discrete states is sufficient. This leads to a linear behavior with temperature: $\langle q_s\rangle^T_{cent} = a_s T$, where the proportionality constant depends on known quantities such as the harmonic frequency ω_s and the equilibrium moment of inertia. Thus,

$$\langle q_s\rangle^T = -\{3k_{sss}\coth(hc\omega_s/2kT) + \sum_{s'} g_{s'} k_{ss's'}\coth(hc\omega_{s'}/2kT)\}/2\omega_s + a_s T \quad (8)$$

Similarly, from the expectation value of q^2 for a vibrational state, $\langle q_s^2\rangle_v = (1/g_s)(v_s + g_s/2)$, one gets the thermal average $\langle q_s^2\rangle^T = \tfrac{1}{2}\coth(hc\omega_s/2kT)$. Thus, we obtain the expectation value for the nuclear shielding as (68)

$$\begin{aligned}\langle\sigma\rangle_v = \sigma_e &+ \sum_s(\partial\sigma/\partial q_s)_e\{-[3k_{sss}(v_s + \tfrac{1}{2})\\ &+ \sum_{s'} g_{s'} k_{ss's'}(v_{s'} + g_{s'}/2)]/\omega_s + \langle q_s\rangle_v^{cent}\}\\ &+ \tfrac{1}{2}\sum_s(\partial^2\sigma/\partial q_s^2)_e(v_s + g_s/2)/g_s + \ldots \quad (9)\end{aligned}$$

for a given vibrational state, with the first sum over s being restricted to totally symmetric modes. The thermal average of the nuclear shielding is then (68)

$$\begin{aligned}\langle\sigma\rangle^T = \sigma_e &+ \sum_s(\partial\sigma/\partial q_s)\{-[3k_{sss}\coth(hc\omega_s/2kT)\\ &+ \sum_{s'} g_{s'} k_{ss's'}\coth(hc\omega_{s'}/2kT)]/2\omega_s + a_s T\}\\ &+ \tfrac{1}{4}\sum_s(\partial^2\sigma/\partial q_s^2)_e\coth(hc\omega_s/2kT) + \ldots \quad (10)\end{aligned}$$

The effects of intramolecular dynamics on nuclear resonance can be interpreted quantitatively, provided that the intramolecular potential function, i.e., the anharmonic force field, of a molecule is known (69). The derivatives of nuclear shielding $(\partial\sigma/\partial q_i)_e$ at the equilibrium configuration of the molecule can be obtained as empirical parameters from precisely measured values of $\langle\sigma\rangle^T - \langle\sigma\rangle^{300}$. Conversely, given the variation of nuclear shielding with configuration, the temperature dependence of nuclear resonance in the independent molecule can be quantitatively predicted (53,70,71).

For the comparison of isotopically substituted molecules, the derivatives $(\partial\sigma/\partial q_i)_e$ which are mass dependent (since the normal coordinates are mass dependent) are not very useful. Instead we can transform Equation (6) to internal coordinates which are mass independent. These transformations are well known from methods of vibrational analysis (72). For a diatomic molecule, there is only one normal coordinate and the result is simple

$$\langle\sigma\rangle^T = \sigma_e + (\partial\sigma/\partial\Delta r)_e\langle\Delta r\rangle^T + \tfrac{1}{2}(\partial^2\sigma/\partial\Delta r^2)_e\langle(\Delta r)^2\rangle^T + \ldots \quad (11)$$

or

$$\langle\sigma\rangle^T = \sigma_e + (\partial\sigma/\partial\xi)_e\langle\xi\rangle^T + \tfrac{1}{2}(\partial^2\sigma/\partial\xi^2)_e\langle\xi^2\rangle^T + \ldots \quad (12)$$

where $\Delta r = R - R_e$, and a reduced coordinate may be defined as $\xi = (R-R_e)/R_e$. Application of Equation (10) then leads to (73)

$$<\sigma>^T = \sigma_e + [(\partial^2\sigma/\partial\xi^2)_e - 3a(\partial\sigma/\partial\xi)_e](B_e/2\omega)\coth(hc\omega/2kT) + \ldots \quad (13)$$

Here, B_e is the rotational constant, and a is the cubic force constant in this reduced coordinate. For nearly all diatomic molecules, the parameter a is of the order of −2 to −4 (74). Thus, the second derivative $(\partial^2\sigma/\partial\xi^2)_e$ would have to be 6 to 12 times as large as the first derivative $(\partial\sigma/\partial\xi)_e$ for the two terms to be comparable in magnitude. Unless we find this to be the case, we can probably safely assume that the first derivative term alone is a sufficiently good approximation.

For a bent triatomic molecule, the bond-angle deformation must also be considered

$$<\sigma>^T = \sigma_e + (\partial\sigma/\partial\Delta r_1)_e<\Delta r_1>^T + (\partial\sigma/\partial\Delta r_2)_e<(\Delta r_2)^2>^T + (\partial\sigma/\partial\Delta\alpha)_e<\Delta\alpha>^T + \ldots \quad (14)$$

For a symmetrical molecule AX_2, the mean bond displacements are identical.

$$<\sigma>^T = \sigma_e + [(\partial\sigma/\partial\Delta r_1)_e + (\partial\sigma/\partial\Delta r_2)_e]<\Delta r>^T + (\partial\sigma/\partial\Delta\alpha)_e<\Delta\alpha>^T \quad (15)$$

If the A nucleus is being observed, the derivatives are equal, but if the X nucleus is being observed, $(\partial\sigma_{X1}/\partial\Delta r_1)_e$ is much larger than $(\partial\sigma_{X1}/\partial\Delta r_2)_e$ and only the sum can be obtained as an empirical parameter. $<\Delta r>$ and $<\Delta\alpha>$ for bent triatomic molecules can be calculated from available anharmonic force fields (75)

$$<\Delta r>^T = (\overline{L}_{11}<q_1>^T + \overline{L}_{12}<q_2>^T)/\sqrt{2}$$

$$r_e<\Delta\alpha>^T = (\overline{L}_{21}<q_1>^T + \overline{L}_{22}<q_2>^T)/\sqrt{2}$$

$\overline{L}_{ij}$ are the transformation constants involving the atomic masses and $<q_1>^T$ and $<q_2>^T$ are evaluated as shown in Equation (8) from cubic force constants $k_{ss's'}$ and harmonic frequencies ω_s, s referring to the totally symmetric modes 1 and 2.

Triatomics are a set of molecules for which least-squares analysis of spectroscopic data can yield the cubic force constants. There are six vibration-rotation constants which appear in the expansion of the rotational constant B_v. These vibration-rotation constants have known relations to cubic force constants $k_{ss's''}$ (76). By measuring B_v in excited vibrational states by microwave spectroscopy, one can get the six vibration-rotation constants and from the latter one can calculate the six unknown $k_{ss's''}$ constants (77).

For a tetrahedral molecule, AX_4, the expression for the thermal average of nuclear magnetic shielding is equally simple (78)

$$<\sigma>^T = \sigma_e + p<\Delta r>^T + \ldots \quad (16)$$

where p is a parameter which is the sum $\sum^4(\partial\sigma/\partial\Delta r_i)_e$. The mean bond angle deformation $<\Delta\alpha>^T$ vanishes here as well as in the planar AX_3 and octahedral AX_6 molecules. The mean displacement $<\Delta_r>^T$ for tetrahedral AX_4, planar AX_3, and octahedral AX_6 molecules is simply related to Equation (8)

$$<\Delta r>^T = (h/4\pi^2c\omega_1nm_X)^{1/2}<q_1>^T \quad (17)$$

where $n = 3,4$, or 6, the quantities q_1 and ω_1 refer to the totally symmetric mode, and m_X is the atomic mass of X. For the simple cases we have considered above, one or two empirical parameters must be determined, $p = \sum^n(\partial\sigma/\partial\Delta r_i)_e$ and $(\partial\sigma/\partial\Delta\alpha_i)_e$, provided the quadratic terms are relatively small in the polyatomic molecule as in the diatomic ones.

The calculation of the mean displacements $<\Delta r>^T$ for simple molecules depends on the availability of the anharmonic force field for the molecule, in particular the harmonic frequencies and the cubic force constants (69). The quartic force constants do not appear in $<\sigma>^T$ until the third-derivative terms in the expansion are considered (79). The problem in determining the general force field for molecules with four or more atoms is that one cannot expect to obtain sufficient spectroscopic data to determine all k constants uniquely. For example, while the six independent cubic k constants can be determined uniquely from six independently measured vibration-rotation constants in bent AX_2 molecules, for pyramidal AX_3 molecules the 14 cubic k constants cannot be uniquely determined from 8 vibration-rotation constants and two ℓ-type doubling constants currently available (69). Nor is it likely that the use of isotopic data will be sufficiently effective to overcome this difficulty. Hence the experimental information has to be supplemented by model functions.

There are two basic types of contributions to the cubic force constants (80). One arises from quadratic force constants in internal coordinates through the nonlinear transformation from internal to normal coordinates. This transformation is nonlinear because the basic assumption of infinitesimal amplitudes in harmonic calculations is no longer valid in anharmonic calculations. Since not only linear terms need to be evaluated in the latter, the instantaneous values of these coordinates rather than their projections on the equilibrium positions must be noted. Thus, a force field which includes only quadratic terms when expressed in the true curvilinear coordinates may involve all anharmonic terms (cubic, quartic, etc.) when transformed into normal coordinates (81).

The second contribution arises from cubic force constants in internal coordinates which may be included by the adoption of model functions. For example, a Morse function may be used for the valence-bond-stretching potential and a Buckingham or Lennard-Jones potential may be used for nonbonded interactions. The adoption of a model function V implicitly defines a cubic force constant ($\partial^3 V/\partial r^3$). Such a model has been used by Kuchitsu and Bartell (80). Other model potentials proposed by Machida and Overend (82) and by Parr and Brown (83) offer promising results (69).

For molecules with 4 or more atoms, one starts by finding an approximate potential function using the quadratic force field for the molecule augmented with model functions, and then refines it further by measurement of other observables such as vibrational band intensities or dipole moments for individual vibrational states. Both these quantities depend on the precise vibrational wavefunction and thus on the precise intramolecular potential functions. The availability of cubic force constants is increasing as results of spectroscopic measurements such as the observation of the Stark effect of lines in vibrational-rotational spectra using ultra-high-resolution laser spectroscopic techniques (84), the intensities of overtone and combination bands observed in the infrared (85), and vibrational circular dichroism (86) become available. At the same time, anharmonic force fields are emerging from *ab initio* calculations (87-89). These sources are complementary. At least some of the theoretically predicted force constants in a molecule are considered more reliable than the experimentally derived values, particularly some of the cubic and quartic constants which are not determined well at all from the analysis of experimental data.

Some mean displacements of atoms from equilibrium positions, $\langle\Delta r\rangle_v$, $\langle\Delta\alpha\rangle_v$, calculated from *ab initio* theory for specific vibrational levels, are known in Table 4 for H_2O (87). The vibrational levels (v_1, v_2, v_3) show an increase in $\langle\Delta r\rangle_v$ with an increasing vibrational quantum number. On the other hand $\langle\Delta\alpha\rangle_v$ increases with increasing quantum number in the case of excitation of the bending mode, although it decreases slightly with increasing vibrational quantum number in excitation of the symmetric stretching mode.

Table 4. Mean Displacements for Some Vibrational States of H_2O, Calculated by a Variation-Perturbation Approach (87)

$v_1\ v_2\ v_3$	$\langle\Delta r\rangle_v$, 10^{-2} Å	$\langle\Delta\alpha\rangle_v$, 10^{-1} deg
0 0 0	1.474	1.23
1 0 0	2.926	−2.12
2 0 0	4.379	−5.47
3 0 0	5.831	−8.8
0 1 0		13.73
0 2 0		26.22
0 3 0		38.7

Table 5. Mean Displacements in Some Small Molecules, Å*

	$\langle\Delta r\rangle^{300}$	$(\langle\Delta r\rangle^{400}-\langle\Delta r\rangle^{200})$ x 10^4	$(\langle\Delta r\rangle_D - \langle\Delta r\rangle_H)$ x 10^4
H_2O	0.0151	5.9	-36.9
D_2O	0.0114	4.9	
H_2S	0.0167	7.0	-40.1
D_2S	0.0127	6.6	
H_2Se	0.0166	7.6	-41.8
D_2Se	0.0125	7.8	
SO_2	0.0045	3.4	
$^{35}ClO_2$	0.0050	5.1	
$^{15}NO_2$	0.0047	3.3	
C-H, CH_3F	0.0108	1.0	
C-F, CH_3F	0.0060	8.4	
CH_4	0.0170	3.5	
BF_3	0.0097	4.2	
$^{14}NH_3$	0.0120	2.5	-17.9
$^{14}ND_3$	0.0102	1.5	
PH_3	0.0175	6.0	-46.3
PD_3	0.0129	6.8	

*Calculated using anharmonic force fields from the following sources: All AX_2-type molecules, K. Kuchitsu and Y. Morino, *Bull. Chem. Soc. Japan* **38**, 814 (1965); CH_3F, M.L. La Boda and J. Overend, *Spectrochim. Acta* **32a**, 1033 (1976); CH_4, K. Kuchitsu and L. S. Bartell, *J. Chem. Phys.* **36**, 2470 (1962); BF_3, C.J. Jameson, *J. Chem. Phys.* **67**, 2814 (1977); NH_3, Y. Morino, K. Kuchitsu and S. Yamamoto, *Spectrochim. Acta* **24a**, 335 (1968); PH_3, K. Kuchitsu, *J. Mol. Spectrosc.* **7**, 399 (1961).

Table 5 shows some mean displacements, $\langle\Delta r\rangle^T$, calculated from available force fields. Note that $\langle\Delta r\rangle^T$ increases with increasing temperature and is larger for the lighter isotopomer. There is considerable experimental evidence that the average bond distances are shortened upon heavy isotope substitution (90). However, there is very little information about the effect of isotopic substitution on bond angle. To prove unambiguously that a given bond angle decreases upon heavy isotope substitution, there must be sufficient spectroscopic data so that no assumptions need be made about any of the bond lengths or bond angles.

Although the mean displacement due to centrifugal distortion is generally small (less than 20% of the total $\langle\Delta r\rangle$), it could be responsible for a large part of the temperature dependence of σ_0. The contribution of anharmonic vibration depends on the function coth ($hc\omega/2kT$). For temperatures between 250 and 400 K, at which NMR measurements in the gas phase are usually carried out, coth ($hc\omega/2kT$) is approximately constant for $\omega > 1500$ cm^{-1}, varies nonlinearly with T for ω between 300 cm^{-1} and 1500 cm^{-1}, and varies linearly with T for $\omega < 300$ cm^{-1}.

Thus, the temperature dependence of σ_0 in tightly bound diatomic molecules like CO, HBr and HCl is almost entirely due to centrifugal distortion. Table 6 compares the relative fractions of the temperature dependence of $\langle\Delta r\rangle^T$ due to anharmonic vibration and centrifugal distortion. Note that the vibrational contribution becomes dominant in the polyatomic molecules, which have several vibrational modes at least some of which have low frequencies. A good example is SF_6, in which an experimental measurement of the variation of the mean S-F bond length with temperature from 298 to almost 1000 K has been reported (91). Of the observed change $\langle\Delta r\rangle^{1000} - \langle\Delta r\rangle^{298} = 0.0065$ Å, only a minor fraction (less than 8%) was due to the rotational contribution. The remainder was adequately reproduced by the calculated anharmonic vibration contribution (92).

Table 6. Summary of Vibrational Contributions to Chemical Shift (78)

Molecule	Temperature range, K	Total chemical shift (calc.), ppm	Anharmonic vibration, %*	ω cm^{-1}
$^{12}CF_4$	270-410	0.766	83	
$^{28}SiF_4$	270-390	0.446	67	
$^{11}BF_3$	290-410	0.341	51	
^{35}ClF	280-350	1.033	47	786.1
F_2	220-350	3.937	36	917.1
^{13}CO	220-380	0.050	1	2121

*Since only linear terms are considered here, the centrifugal distortion contribution is the remaining fraction.

2. Variation of Nuclear Magnetic Shielding with Molecular Geometry

Using $\langle\Delta r\rangle^T$ values such as those shown in Table 5, one can compare the experimental $\langle\sigma\rangle^T - \langle\sigma\rangle^{300}$ shown in Figures 7 and 8 with the calculated functions

$$\langle\sigma\rangle^T - \langle\sigma\rangle^{300} = (\partial\sigma/\partial\Delta r)_e\,[\langle\Delta r\rangle^T - \langle\Delta r\rangle^{300}] + (\partial\sigma/\partial\Delta\alpha)_e[\langle\Delta\alpha\rangle^T - \langle\Delta\alpha\rangle^{300}] + \ldots \quad (18)$$

Here the unknown parameters $(\partial\sigma/\partial\Delta r)_e$ and $(\partial\sigma/\partial\Delta\alpha)_e$ can be empirically determined by a best fit to the experimental curves. For ^{19}F in CF_4, the parameter obtained is the sum of four derivatives which could probably be interpreted almost entirely as $(\partial\sigma^{F_1}/\partial\Delta r_1)_e$, the derivative of the ^{19}F shielding with respect to that stretch of that C-F bond which involves that particular F nucleus rather than the stretch of the neighboring C-F bonds (78). An example of the comparison between experimental and theoretical (one-parameter fit) curves is shown in Figure 10. Note that the centrifugal distortion contribution to $\langle\Delta r\rangle^T$ is linear, whereas the anharmonic vibration contribution has noticeable curvature. The nonlinear behavior of the vibrational portion of $\langle\Delta r\rangle^T$ depends on the behavior of the function coth ($hc\omega/2kT$). For polyatomic molecules, a linear combination of coth functions determines the curvature of $\sigma_0(T)$.

Table 7 shows empirical values of derivatives of nuclear shielding with respect to bond extension obtained by this one-parameter fitting procedure. The empirical derivatives are all negative, which may be a general trend for ^{19}F shielding. In the same table are some derivatives taken from coupled Hartree-Fock and variational calculations of nuclear shielding in diatomic molecules (70,71,93-98). Except for ^7Li in LiH, these theoretical derivatives are also negative.

A simplistic picture can help to understand these findings. Nuclear magnetic shielding in a molecule has two parts, a positive diamagnetic term which generally decreases as the internuclear separation increases (99), and a negative paramagnetic term roughly related to the deviation of the charge

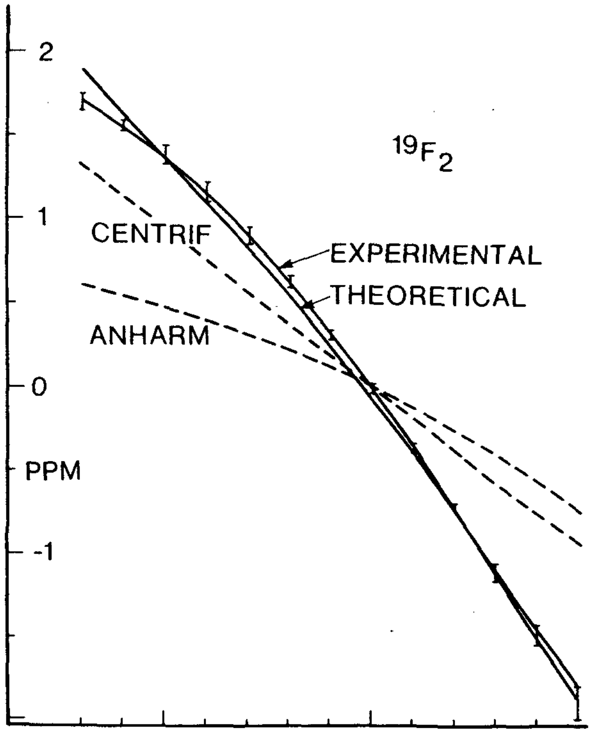

Figure 10. Comparison of experimental and theoretical temperature dependence of nuclear shielding for ^{19}F in F_2, showing separate contributions of anharmonic vibration and centrifugal distortion (68).

Table 7. Empirical and Theoretical Derivatives of Magnetic Shielding

	$(\partial\sigma/\partial\Delta r)_e$, ppm/Å Empirical	Theoretical	Reference
^{19}F in F_2	−4530		68
^{19}F in ClF	−2073		68
^{19}F in CF_4	−1115[1]		78
^{19}F in SiF_4	−1170[1]		78
^{19}F in BF_3	−1115[1]		78
^{13}C in CO	−240	−413.7	68,93[2]
^{1}H in HBr	−400		56
^{1}H in HCl	−78.2		57
^{1}H in H_2		−21.8	96
^{1}H in LiH		−2.69	70[2]
^{1}H in HF		−40.7	71[2]
^{7}Li in LiH		+7.51	70[2]
^{15}N in N_2		−640.5	94[2]
^{17}O in CO		−479	93[2]
^{19}F in HF		−411	71[2]

[1] This empirical value is for the sum $(\partial\sigma^{F1}/\partial\Delta r_1)_e + (\partial\sigma^{F1}/\partial\Delta r_2)_e + (\partial\sigma^{F1}/\partial\Delta r_3)_e + \ldots$. However, $(\partial\sigma^{F1}/\partial\Delta r_1)_e$ will be the dominant contribution.

[2] Derivatives from (70), (71), (93), and (94) were obtained by fitting a parabola to theoretical σ values at three distances.

distribution from spherical symmetry (100). Studies of charge-distribution maps of diatomic molecules have shown that the relaxation of the molecular charge density caused by the extension of the bond removes charge from along the internuclear axis and concentrates it in the perpendicular region (101). The quadrupolar character of the relaxation of charge density is most pronounced for the N, O and F nuclei in molecules such as N_2, CO, BF, LiF, and BeO. Charge-distribution difference maps illustrating this are reproduced in Figure 11 for LiF and N_2. In terms of *p* orbital populations, this charge redistribution is equivalent to a decrease in p_z population accompanied by an increase in p_x and p_y populations. In the model of Saika and Slichter, these changes in orbital populations lead to a larger negative paramagnetic contribution to ^{19}F shielding in these molecules (100). On the other hand, the charge-density-difference maps have also shown that upon bond extension the charge polarization in the vicinity of the Be and Li nuclei in BeF and LiF is primarily dipolar. The charge density is removed from the overlap region and builds up immediately in front of the Li or Be nucleus, that is, valence charge density is transferred from F back to Li in LiF with bond extension (101). In the Saika and Slichter model, this could lead to increased ^7Li shielding. This is a simplistic picture, of course. A more detailed theoretical study of the change in nuclear magnetic shielding with internuclear separation is required.

The variation of nuclear shielding with angle deformation has been explored to some extent (102). For ^{31}P shielding in PZ_3 molecules, Letcher and Van Wazer have shown that the sigma contribution to the paramagnetic term (pi contributions were considered separately) varied with the ZPZ bond angle. Their results indicate that ^{31}P in PZ_3 molecules with ligands Z (such as H or F) which are more electronegative than P would show a negative $(\partial\sigma/\partial\Delta\alpha)$. From their calculations for electronegativity of *Z* equal to 4.0 (e.g., PZ_3 = PF_3), we find that the predicted angular dependence corresponds to $(\partial\sigma/\partial\Delta\alpha) = -64$ ppm/deg. Although the diamagnetic term in σ is not included, the resulting variation of σ with angle deformation is probably correct, since ^{31}P changes in σ are known to be dominated by the paramagnetic term (102).

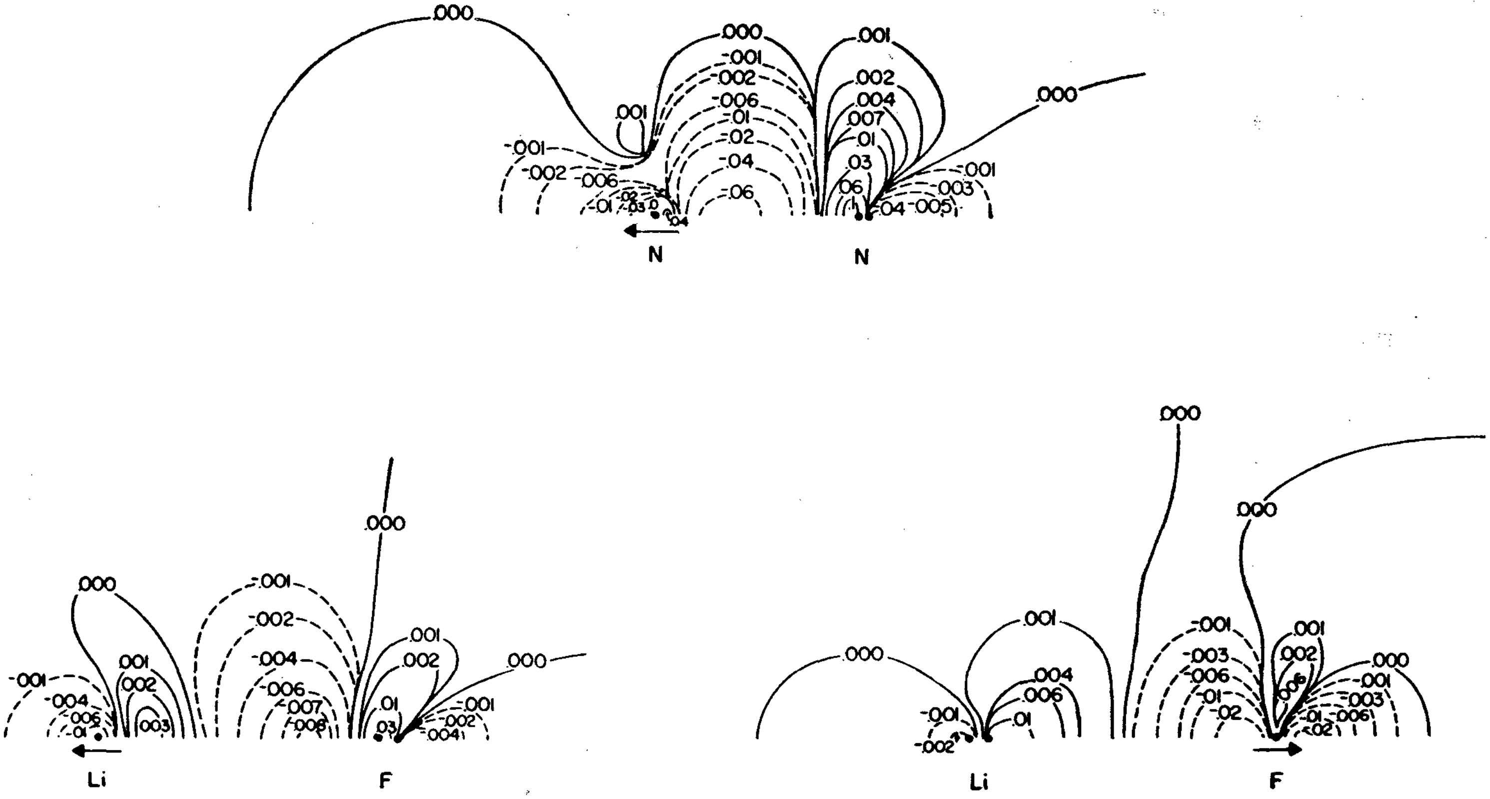

Figure 11. Charge redistribution upon bond extension in LiF and N_2 molecules, from Bader and Bandrauk (101). Positive contours correspond to an increase, negative contours to a decrease in electronic charge density. Displacement of nucleus marked by arrow is 0.132 a.u. for N_2, 0.232 a.u. for LiF.

The change in the diamagnetic part of the shielding accompanying changes in bond angle has been calculated by Bernheim and Batiz-Hernandez (103). For protons in CH_3X (X = H,D) in which the C-H bond distance was assumed constant and the HCH angle was allowed to vary from 105 to 115 degrees, σ^d was found to vary from 30.774 to 29.927 ppm. Similar calculations were carried out for NH_3. The diamagnetic part of the shielding changed from 33.868 to 32.566 ppm as the HNH angle was changed from 100 to 110 degrees. If only the diamagnetic term is considered, these calculations both give a negative $(\partial\sigma/\partial\Delta\alpha)_e$, −0.0847 ppm/deg and −0.130 ppm/deg for CH_3X and NH_3, respectively. These numbers may be in error by as much as a factor of two, since the paramagnetic term may not be negligible for protons (104).

As yet, there is no theoretical study of $(\partial\sigma/\partial\Delta\alpha)$ at the same quantitative level as the theoretical results shown in Table 7. Likewise empirical values for $(\partial\sigma/\partial\Delta\alpha)_e$ are not yet generally available. The problem lies in calculating $\langle\Delta\alpha\rangle^T$ for a molecule. This depends strongly on bending cubic force constants which are less reliable than the ones used in calculating $\langle\Delta r\rangle^T$, primarily due to lack of a model analogous to the Morse function.

C. Isotope Effects in NMR

Anharmonic vibration and centrifugal distortion cause bond lengths and bond angles to depend on isotopic mass, as illustrated in Figure 9. The concomitant change in nuclear shielding upon bond displacement or bond-angle distortion results in the observed isotope shift in NMR. The heavier molecule sits lower in the potential curve and thus experiences a smaller mean displacement from the equilibrium geometry. For example, deuterium substitution shortens the average bond length by 0.003-0.005 Å, whereas isotopic substitution by heavier atoms, such as replacement of ^{32}S by ^{34}S, shortens it by about 0.0001 Å (90). Since nuclear shielding generally decreases with bond extension, as seen in the previous section, the resonant nucleus in the heavier molecule experiences on the average greater shielding than does the nucleus in the lighter molecule.

1. General Observations

A very large number of isotope shifts in NMR have been reported. Batiz-Hernandez and Bernheim (105) give a useful review of results prior to 1967. They make the following general observations about the magnitudes and directions of the isotope shifts:

(1) Heavy isotopic substitution shifts the NMR signal of a nearby nucleus toward a higher magnetic field.

(2) The magnitude of the isotope shift depends on how remote the isotopic substitution is from the nucleus under observation.

(3) The magnitude of the shift is a function of the resonant nucleus, reflecting the differences in the range of chemical shifts observed for the nuclei.

(4) The magnitude of the shift is largest where the fractional change in mass upon substitution is largest.

(5) The magnitude of the shift is approximately proportional to the number of atoms in the molecule that have been substituted by isotopes.

Table 8 gives examples of the magnitudes of the shifts and illustrates general observations (3) and (4). Observation (2) provides an advantage, for example, in the ^{18}O-induced ^{31}P shifts where ^{18}O substitution results in observable shifts only for adjacent ^{31}P nuclei (106,107). Shifts in the ^{31}P nuclei farther removed from the ^{18}O substitution site in the same molecule were too small to be resolved. Observation (5) is most striking in the case of ^{59}Co shifts resulting from deuterium substitution in $[Co(en)_3]Cl_3$. Bendall and Doddrell (108) recorded all thirteen peaks corresponding to the members of the isotopic homologous series in which the 12 exchangeable hydrogen atoms per molecule of tris-(ethylenediammine) cobalt(III)chloride are replaced by deuterium atoms. In Figure 12 from their paper, the peaks appear equally spaced, within experimental error, and unequivocally show a proportionality of the isotope shift to the number of atoms which have been substituted. The isotope shifts in ^{13}C of $CH_{4-n}D_n$, ^{15}N of $NH_{3-n}D_n$ and ^{31}P of $PH_{3-n}D_n$ also show the same approximate proportionality (109-111).

Table 8. Magnitudes of Secondary Isotope Shifts in ppm per D Atom or other Isotope Substituted[1]

Resonant nucleus	(^1H, ^2D)	(^{16}O, ^{18}O)	(^{12}C, ^{13}C)	(^{32}S, ^{34}S)
^1H	0.012-0.040		0.002-0.005[2]	
^{13}C	0.043-0.296[3]	0.035[4]	0.01-0.03[5]	0.009[6]
^{17}O	1.54			
^{19}F	0.21-0.50		0.072-0.192	0.033-0.053[7]
^{31}P	0.85[8]-1.30[9]	0.0166-0.0285[10]		
^{59}Co	5.2[11]		0.915	
Fractional change in mass, %	100	12.5	8.33	6

[1] Data from compilation of Batiz-Hernandez and Bernheim (105) unless indicated otherwise.

[2] E.A.V. Ebsworth and J.J. Turner, *J. Chem. Soc., Faraday Trans.* **60**, 256 (1964).

[3] Yu.K. Grishin, N.M. Sergeyev and Yu.A. Ustynyuk, *Mol. Phys.* **22**, 711 (1971).

[4] J.M. Risley and R.L. Van Etten, *J. Am. Chem. Soc.* **101**, 252 (1979).

[5] F.J. Weigert and J.D. Roberts, *J. Am. Chem. Soc.* **94**, 6021 (1972).

[6] S.A. Linde and H.J. Jakobsen, *J. Magn. Reson.* **17**, 411 (1975).

[7] R. Gillespie and J.W. Quail, *J. Chem. Phys.* **39**, 2555 (1963).

[8] (111).

[9] A.A. Borisenko, N.M. Sergeyev, and Yu.A. Ustynyuk, *Mol. Phys.* **22**, 715 (1971).

[10] (107).

[11] (108).

2. Interpretation of Isotope Effects

Since the temperature dependence of nuclear shielding in the isolated molecule and the isotope effect on nuclear shielding both result from the vibrational and rotational effects, it should be possible to explain isotope effects with the same theoretical framework used to explain temperature effects on nuclear resonance (112,113).

For diatomic molecules, it is relatively simple to express the explicit dependence of the isotope shift due to anharmonic vibration on the reduced mass of the molecule. If we ignore the term involving the second derivative, for reasons stated earlier, the shielding in a diatomic molecule can be written as

$$<\sigma>^T = \sigma_e + [f_{anh}(T) + f_{rot}(T)](\partial \sigma / \partial \Delta r)_e \ldots \qquad (19)$$

In the diatomic molecule the rotational contribution is a very simple one and is easily seen to be independent of isotopic replacement (112). Thus, we find (113)

$$<\sigma^i>^T - <\sigma>^T =$$

$$f_{anh}(T)(\partial \sigma / \partial \Delta r)_e \left[\left(\frac{\mu^i}{\mu} \right)^{-1/2} \frac{\coth(hc\omega^i / 2kT)}{\coth(hc\omega / 2kT)} - 1 \right] \qquad (20)$$

In most cases (but notably not for hydrogen isotopes), the ratio μ^i/μ is close to unity, in which case, $(\mu^i/\mu)^{-1/2}$ is approximately $-(\mu^i-\mu)/2\mu$. If $\coth(hc\omega/2kT)$ is of the order of unity,

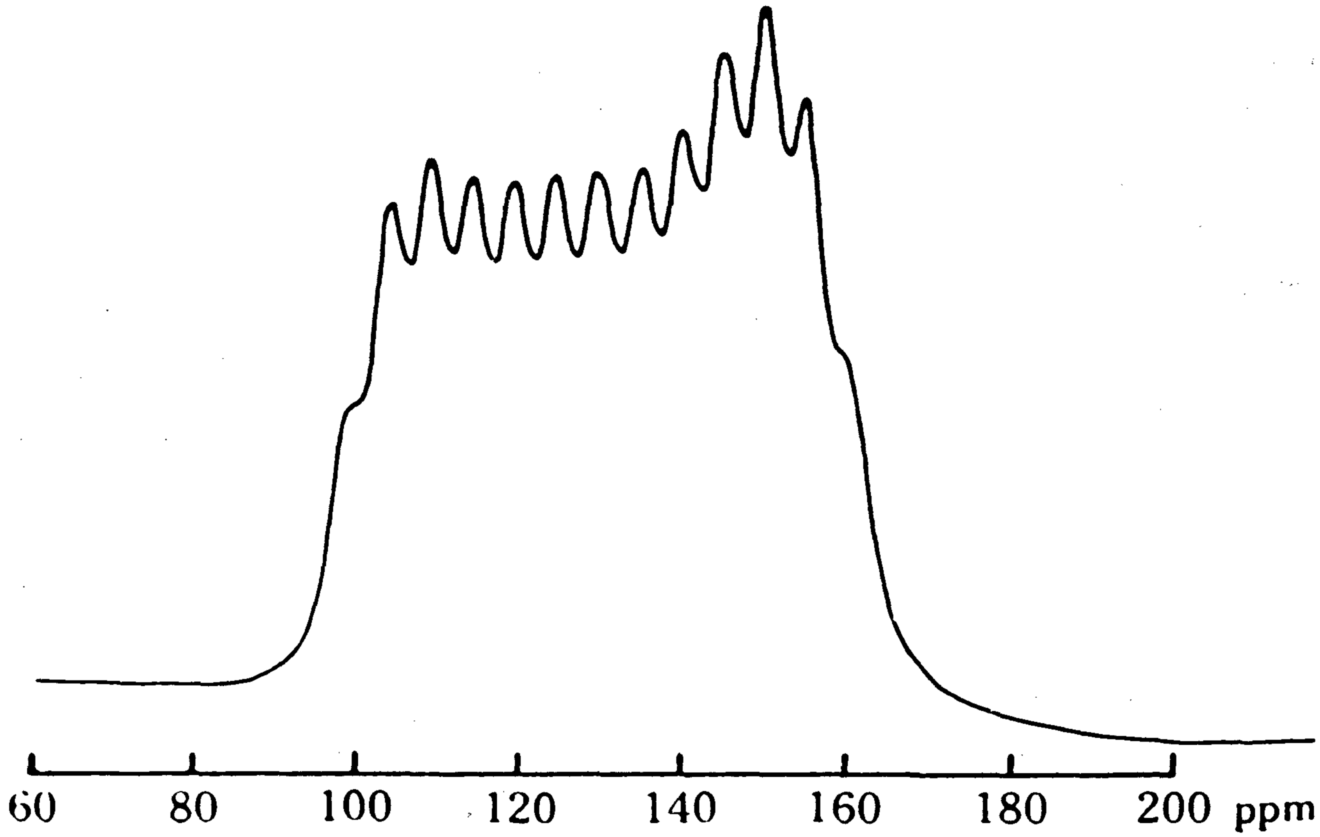

Figure 12. ^{59}Co NMR spectrum in a solution of $[Co(en)_3]Cl_3$ in H_2O/D_2O, showing all 13 peaks corresponding to the members of the isotopic homologous series in which the 12 exchangeable hydrogen atoms per molecule of the cobalt complex are replaced by deuterium atoms, from Bendall and Doddrell (108).

$$\Delta\sigma = <\sigma^i>^T - <\sigma>^T \simeq -[(\mu^i - \mu)/2\mu]f_{anh}(T)(\partial\sigma/\partial\Delta r)_e \quad (21)$$

To this approximation, the magnitude of the isotope shift is proportional to $(\partial\sigma/\partial\Delta r)_e$ in a diatomic molecule. In a polyatomic molecule, it would be related to a linear combination of $(\partial\sigma/\partial\Delta r_j)_e$ and perhaps $(\partial\sigma/\partial\Delta\alpha)_e$.

Using Equation 21, we can explain the general observations of Batiz-Hernandez and Bernheim (105):

(1) *Heavy isotopic substitution shifts the NMR signal of a nearby nucleus toward a higher magnetic field.* In Equation (21), if $(\partial\sigma/\partial\Delta r)_e$ is negative, as is typically the case (Table 7), then for positive $\Delta\mu$, $\Delta\sigma$ is positive: the *resonant* nucleus in the heavier isotopic form is more shielded than the lighter molecule and thus appears at higher magnetic field. For polyatomic molecules the situation is somewhat more complicated but a trend parallel to that predicted by Equation (21) might be expected.

(2) *The magnitude of the isotope shift is dependent on how remote the isotopic substitution is from the nucleus under observation.* For a given molecule and its isotopically substituted counterpart, the quantities $<\Delta r>^T$, $<(\Delta r)^2>^T$, $<\Delta\alpha>^T$, . . ., which are properties of the dynamic state of the molecule, are fully determined at a given temperature. If we now observe different resonant nuclei on the same pair of isotopically related species, then the isotope shift is different for each resonant nucleus only due to differences in $(\partial\sigma/\partial\Delta r)_e$ for the observed nuclei. It is reasonable to expect that the shielding of a resonant nucleus depends to a greater extent on an angle displacement or bond stretch in its immediate vicinity in the molecule, and that it depends to a lesser extent on an internal coordinate further removed from it. That is, $(\partial\sigma/\partial\Delta r_j)_e$ is expected to be smaller for an internal coordinate Δr_j which is farther from that nucleus, thus leading to a smaller isotope shift for the nucleus more remote from the substitution site.

(3) *The magnitude of the shift is a function of the resonant nucleus, reflecting the differences in the range of chemical shifts observed for the nuclei.* There are general trends in the range of chemical shifts of nuclei. The range increases roughly with increasing atomic number (114). In an approximate theory of nuclear magnetic shielding that takes into account only the electrons in orbitals centered on the nucleus in question, the dependence on atomic number of the magnitudes of the range of chemical shifts can be explained on the basis of the extent of deviations from spherical symmetry of the electron distribution with increasing atomic number, and the periodic changes in $<r^{-3}>$ for atoms across the periodic table (115). Whereas the range of chemical shifts is a measure of the change in σ accompanying changes in nuclear environment from one molecule to another, the $(\partial\sigma/\partial\Delta r)_e$ are measures of the change in σ with relatively minor departures from the equilibrium molecular configuration. The nuclear species with a larger range of chemical shifts is expected to have larger derivatives $(\partial\sigma/\partial\Delta r)_e$ as well. If we now consider observing resonant nuclei of different kinds of atoms, e.g., ^1H and ^{19}F, in the same pair of isotopically related molecules, the properties of the dynamic state are set and the isotope shift is different for each nucleus only due to differences in $(\partial\sigma/\partial\Delta r)_e$. The generally larger derivatives for σ of a resonant nucleus whose range of chemical shifts is large lead to a larger isotope shift.

(4) *The magnitude of the shift is largest where the fractional change in mass upon isotopic substitution is largest.* For a given resonant nucleus in a diatomic molecule, $(\partial\sigma/\partial\Delta r)_e$ is fixed. Equation (21) shows that the isotope shift is proportional to $(\mu^i-\mu)/\mu$. Thus, the isotope shift between $^1H^3T$ and $^1H_2$ is greater than that between $^1H^2D$ and $^1H_2$ (96). In polyatomic molecules, the situation is more complex but it is to be expected that the mass-dependent terms also lead to isotope shifts related to $(m^i-m)/m$. Thus, we should expect that the largest isotope shifts occur with the largest fractional change in mass upon isotopic substitution in polyatomic molecules as well.

(5) *The magnitude of the shift is approximately proportional to the number of atoms in the molecule that have been substituted by isotopes.* In comparing the isotopic homologs $^{13}C^{16}O_2$, $^{13}C^{16}O^{18}O$, and $^{13}C^{18}O_2$ using the theory presented in section B1, excluding the terms in the second derivative, it was found that the calculated increase in shielding in this series is approximately linear (113). Lauterbur (116) has noted that this observation in NMR isotope shifts may be related to the observation by Bernstein and Pullin (117) of an approximate linear relation of the zero-point energy of isotopic homologs to the number of equivalent isotopic substituents. Wolfsberg has employed perturbation theory to rationalize the approximate validity of the linear relation and to point out some of the factors that influence this validity (118). This linear increase of the zero-point energy in an isotopic homologous series with an increase in the number of equivalent heavy isotopic substituents, is expected to be accompanied by a decrease in the mean bond lengths with increasing number of heavy substituents, in the same way that a single isotopic *substitution* by a successively heavier atom is accompanied by a successive decrease in the mean bond length in a diatomic molecule (see Figure 9). An approximate linear relation of the mean bond lengths of isotopic homologs to the number of equivalent isotopic substituents has not yet been observed and would be very difficult to establish since it is usually necessary to combine spectroscopic data from several isotopic species in the calculation of the average structural parameters of a molecule (104, 119, 120).

In explaining the general observations on NMR isotope shifts noted by Batiz-Hernandez and Bernheim, we have considered only the isotope effect on the term involving anharmonic vibration. The rotational (centrifugal distortion) contribution and the contributions due to harmonic vibration which involve the second derivatives, $(\partial^2\sigma/\partial(\Delta r)^2)_e$ have not been included. We have yet to determine if either of these neglected contributions can largely account for the observed isotope shifts, and if so, to what extent they can be used to explain the five general observations.

Let us dispose of centrifugal distortion first. We have already noted that the rotational contribution to the mean displacement in diatomic molecules is mass independent. Therefore, there will be no rotational contribution to the isotope shift in any diatomic molecule. For polyatomic molecules with a high degree of symmetry, the rotational contribution to the isotope shift is zero if substitution is made symmetrically. This is based on the mass-independent centrifugal distortion in these molecules, as shown by Toyama *et al* (66). For example, the rotational contribution to shielding for a

CH_4-type molecule is $(3kT/4r_eF_{11})(\partial\sigma/\partial\Delta r)_e$, in which F_{11} is the symmetric stretch quadratic force constant. Similar expressions hold for CO_2-, BF_3- and SF_6-type molecules. Since the force constants F_{ij} and the derivatives $(\partial\sigma/\partial\Delta r)_e$ are independent of isotopic substitution in the context of the Born-Oppenheimer approximation, so are the rotational contributions to σ, if isotopic substitution preserves the symmetry. Thus, in these cases any observed isotopic shift comes from anharmonic vibration or the second-order harmonic terms. If centrifugal distortion were to dominate isotope shifts, then the empirically observed proportionality of the shift to the number of atoms substituted would not be observed in molecules of high symmetry. For example, the ^{13}C shift in CH_3D, CH_2D_2, CHD_3, and CD_4 relative to CH_4 would increase with each additional deuterium and then go to zero for CD_4. On the contrary, the ^{13}C shift in this series is found to be linear with the number of deuteriums (109). That behavior of this type has not been observed implies that the centrifugal distortion contribution probably does not dominate isotope shifts, although the rotational contribution to isotope shifts is not necessarily negligible.

The harmonic-vibration contribution to the isotope shift, which involves the second derivatives $(\partial^2\sigma/\sigma(\Delta r)^2)_e$, is also found to be unable by itself to account for the observed trends. Although this contribution is not necessarily small, for example, 31% of the ^{19}F isotope shift in HF-DF comes from this term (53), it does not appear to be dominant. With the great variety of molecules for which isotope shifts are available, one would expect that the magnitudes and signs of the second derivatives of shielding with respect to bond stretches and angle deformations are likely to be very different. There are a great variety of mixed second derivatives possible: a stretch combined with another stretch, a stretch with an adjacent angle, a stretch with an opposite angle, and so on. For example, in the NH_3 molecule there are 6 and in CF_3Cl there are 16 unique second derivatives of σ with respect to internal coordinates. If the terms involving the second derivative were dominant, then the sign of the isotope shift would not be so universally uniform.

The exceptions to observation (1) (isotope shifts are uniformly upfield upon heavy isotope substitution) are rare. Two instances of downfield shifts, that is, increased nuclear shielding accompanying replacement of ^{12}C by ^{13}C, have been reported recently: a 0.14-ppm shift in the ^{119}Cd shielding and a 0.4-ppm shift in the ^{199}Hg shielding by ^{13}C substitution in the dimethyl cadmium and mercury compounds, respectively (121,122). The fact that the isotope shift has been found to be in the same direction in all other cases implies two very general conditions:

(a) The terms in the first derivative nearly always dominate over the higher order terms.

(b) The first derivatives nearly always have the same sign. In Table 7 we noted that empirical and theoretical derivatives $(\partial\sigma/\partial\Delta r)_e$ are negative, with the exception, so far, of ^7Li shielding in LiH (70). Any other conditions would require highly unusual coincidences in each of hundreds of examples of isotope shifts.

We have seen that the general empirical observations regarding isotope shifts in NMR can be explained by the approximate theoretical treatment described here. In some cases, the temperature dependence of chemical shielding is so small as to be within the possible error of measurements at different temperatures. In these instances the isotope shift may be a more reliable method of obtaining an empirical $(\partial\sigma/\partial\Delta r)_e$. Although the molecular property considered here has been the NMR shielding, the theoretical treatment holds for any molecular electronic property such as dipole moment, hyperfine coupling constant, and diamagnetic susceptibility. Each property will have characteristic derivatives with respect to internal displacement coordinates, but all the molecular constants which have to do with the dynamic state of the molecule remain the same. In fact, since the isotope shifts in the other molecular electronic properties are determined by relationships similar to Equation (21), we can predict that observations (4) and (5) will be found in these properties as well.

IV. CONCLUSIONS

In the introduction we mentioned three facets of our interest in temperature, solvent, and isotope effects on NMR chemical shifts. First is the need to know the magnitude and nature of the effects of environment in order to separate its effects properly from those due to the system under study. Second is the use of NMR as a probe of intermolecular forces and intramolecular force fields. Third is the study of nuclear magnetic shielding as a molecular electronic property in its own right.

Empirically, we have obtained the most information about the first. The density and temperature dependence of σ in the gas phase, as well as comparative studies in solution, reveal the nature and magnitude of environmental effects, which Table 3 shows are not necessarily small. We have seen that by proper extrapolation procedures, it is indeed possible to separate out environmental effects. In cases where this is not rigorously possible, there is enough information about the dependence of the shift on the resonant nucleus, the site in the molecule, the shape of the solvent molecule, its polarizability, ionization potential, dielectric constant, and other properties, to permit the preparation of experiments which duplicate the environmental effects on chemical shifts for control studies not involving the system of interest. At the very least, it is possible to estimate how serious a problem the environmental effects pose.

We have the most difficulty with the second. We are not yet ready to extract parameters of intramolecular force fields or intermolecular potential functions from experimental NMR shifts. However, given an intramolecular force field, it may be possible to test its adequacy in some cases. For example, it has been shown that the available anharmonic force field for PH_3 and PD_3 can not account for both the observed temperature dependence (which Figure 8 shows is opposite to all others previously measured) and the observed isotope shift (which has the usual sign) (123).

Information on intermolecular forces comes from very diverse sources (124). This information can be extracted by analysis of measurements of an observable quantity which has some functional dependence on the intermolecular potential. The degree of success depends on the accuracy of the measurements, on the completeness of the theory connecting the potential to the molecular properties measured, and on the sensitivity of this connection. In some cases, the absence of a one-to-one mapping of the potential onto the measured property may preclude derivation of a unique potential from the observable data, however accurate. In each measurable property from which intermolecular forces have been extracted, the intermolecular potential is involved in a way that is somewhat different from other measurable properties. Thus, if one used several very accurate observables, each of which involves the intermolecular potential in some theoretically established way, it would be feasible to obtain the intermolecular potential with some degree of confidence.

The use of NMR as a probe of intermolecular forces basically awaits a reliable general form of $\sigma(R,\theta,\phi)$. Once this is available, the precision and quantity of experimental data derived from two or more nuclei in the molecular pair will be sufficient to determine a multiparameter potential function. However, there is no guarantee that $\sigma(R,\theta,\phi)$ will be any easier to obtain than $V(R,\theta,\phi)$. There is some indication of the difficulty involved in the attempt to obtain $\sigma(R)$ for Xe interacting with Xe. Quantum mechanical calculations do not provide an easy answer since long-range effects on σ are even more difficult to calculate than dispersion energies. The only consolation at this point is that some other methods for determining intermolecular potential functions are not much more successful.

For the third facet of interest, we have very good empirical information, much better than the analogous information on molecular electronic properties of this type, for example, electric polarizability or molecular dipole moment. We are able to obtain information on the σ function itself about the equilibrium configuration because the theory is sound and intramolecular force fields are much better known than intermolecular potential functions. We are able to obtain empirical derivatives $(\partial\sigma/\partial\Delta r)_e$ with greater accuracy and precision than $(\partial\alpha/\partial R)$ or $(\partial\mu/\partial R)$ (125,126).

One important revelation is that comparisons of quantum mechanical σ calculations with experimental chemical shifts have to be done with great care. Magnitudes of vibrational-rotational corrections to σ are shown in Table 9. We see that even in the isolated molecule, experimental results include intramolecular dynamic effects on σ which are not small. Comparison of differences between quantum mechanical σ values and liquid shifts is definitely unwarranted since we have seen that both $\sigma_0(T)$ and $\sigma_1(T)$ can be large.

Table 9. Estimate of Vibrational-Rotational Correction at 300 K

Nucleus	Molecule	$\langle\sigma\rangle^{300}-\sigma_e$, ppm	Reference
^1H	H_2	−0.38	96
	HF	−0.38	53
	HCl	−1.34	57
	HBr	−7.11	56
^{13}C	CO	−1.05	68
^{19}F	HF	−9.75	53
	ClF	−13	68
	F_2	−40	68
	SiF_4	−5.73	78
	CF_4	−7.24	78
	BF_3	−10.82	78
^{31}P	PH_3	+50	123

There is a connection between the intramolecular and intermolecular effects. We observe the shielding function $\sigma(R,\ldots)$ in terms of its ensemble average over all configurations in van der Waals systems, observed as $\sigma_t(T)$ values. On the other hand, we see the shielding function $\sigma(R,\ldots)$ in terms of its derivatives at the equilibrium configuration in covalently bound systems, weighted according to the thermal average of bond extensions and angle deformations in the molecule, observed as $\sigma_0(T)$ or as isotope shifts. It is not yet known whether the forms of these two types of $\sigma(R,\ldots)$ functions are substantially different or fairly similar. Some hope is offered by the fact that $V(R,\ldots)$ for van der Waals molecules are in principle no different from those in covalent molecules as evidenced by the increasing quantity of spectroscopic information on van der Waals molecules (127). Perhaps the same can be said about $\sigma(R,\ldots)$.

ACKNOWLEDGMENT

The cited research from our laboratory has been supported in part by grants from the National Science Foundation, CHE77-09133 and CHE77-09197.

References

[1] A.D. Buckingham and J.A. Pople, *Faraday Soc. Discuss.* **22**, 17 (1956).

[2] W.T. Taynes, A.D. Buckingham, and H.J. Bernstein, *J. Chem. Phys.* **36**, 3481 (1961).

[3] L. Petrakis and H.J. Bernstein, *J. Chem. Phys.* **38**, 1562 (1963).

[4] G. Widenlocher, *Ann. Phys. (Paris)* **1**, 327 (1966).

[5] E. Kanegsberg, B. Pass, and H.Y. Carr, *Phys. Rev. Lett.* **23**, 572 (1969).

[6] A.K. Jameson, C.J. Jameson, and H.S. Gutowsky, *J. Chem. Phys.* **53**, 2310 (1970).

[7] F.H.A. Rummens, *Mol. Phys.* **21**, 535 (1971).

[8] J.G. Oldenziel, Ph.D. Thesis, University of Amsterdam (1972).

[9] F.H.A. Rummens, in *NMR Basic Principles and Progress*, P. Diehl, E. Fluck, and R. Kosfeld, Eds., Springer-Verlag, New York, 1975, Vol. 10, 1-118.

[10] W.T. Raynes, in *Nuclear Magnetic Resonance (Specialist Periodical Reports)*, R.A. Abraham, Ed. The Chemical Society, London, 1979, Vol. 8.

[11] W.C. Dickinson, *Phys. Rev.* **81**, 717 (1951).

[12] C.J. Jameson, A.K. Jameson, and H. Parker, *J. Chem. Phys.* **70**, 5916 (1979).

[13] G. Heckmann and E. Fluck, *Mol. Phys.* **23**, 175 (1972).

[14] C.J. Jameson, A.K. Jameson, H. Parker, S.M. Cohen, and C.L. Lee, *J. Chem. Phys.* **68**, 2861 (1978).

[15] A.A. Bothner-By, *J. Mol. Spectrosc.* **5**, 52 (1960).

[16] D.F. Evans, *Proc. Chem. Soc.* **115** (1958).

[17] S. Mohanty and H.J. Bernstein, *J. Chem. Phys.* **54**, 2254 (1971).

[18] C.J. Jameson, A.K. Jameson, and S.M. Cohen, *J. Chem. Phys.* **59**, 4540 (1973).

[19] C.J. Jameson, A.K. Jameson, and S.M. Cohen, *J. Chem. Phys.* **62**, 4224 (1975).

[20] C.J. Jameson, A.K. Jameson, and S.M. Cohen, *J. Chem. Phys.* **65**, 3401 (1976).

[21] C.J. Jameson, A.K. Jameson, and S.M. Cohen, *J. Chem. Phys.* **66**, 5226 (1977).

[22] C.J. Jameson, A.K. Jameson, and H. Parker, *J. Chem. Phys.* **68**, 3943 (1978).

[23] B. Linder, *J. Chem. Phys.* **33**, 668 (1960).

[24] Ph. de Montgolfier, *J. Chim. Phys.* **64**, 639 (1967).

[25] L. Onsager, *J. Am. Chem. Soc.* **58**, 1486 (1936).

[26] J. Homer, *Appl. Spectrosc. Rev.* **9**, 1 (1975).

[27] A.D. Buckingham, T. Schaefer, and W.G. Schneider, *J. Chem. Phys.* **32**, 1227 (1960).

[28] M.J. Stephen, *Mol. Phys.* **1**, 223 (1958).

[29] J.P. Riley, I.H. Hillier, and W.T. Raynes, *Mol. Phys.* **38**, 353 (1979).

[30] A.J. Sadlej, M. Zaucer, and A. Azman, *Mol. Phys.* **35**, 1397 (1978).

[31] K. Jackowski, W.T. Raynes, and A. J. Sadlej, *Chem. Phys. Lett.* **54**, 128 (1978).

[32] F.M. Mourits, Ph.D. Thesis, University of Regina, Canada, 1978.

[33] A.D. Buckingham, *Can. J. Chem.* **38**, 300 (1960).

[34] T.W. Marshall and J.A. Pople, *Mol. Phys.* **1**, 199 (1958).

[35] J.I. Musher, in *Advances in Magnetic Resonance*, J.S. Waugh, Ed., Academic Press, New York, 1966, Vol. 2, p. 177.

[36] B. Day and A.D. Buckingham, *Mol. Phys.* **32**, 343 (1976).

[37] A.J. Sadlej and W.T. Raynes, *Mol. Phys.* **35**, 101 (1978).

[38] J.G. Batchelor, *J. Am. Chem. Soc.* **97**, 3410 (1975).

[39] A.D. Buckingham and K.P. Lawley, *Mol. Phys.* **3**, 219 (1960).

[40] F.H.A. Rummens, *J. Am. Chem. Soc.* **92**, 3214 (1970).

[41] W.B. Neilsen and R.G. Gordon, *J. Chem. Phys.* **58**, 4149 (1973).

[42] N.J. Bridge and A.D. Buckingham, *Proc. R. Soc. London, Ser. A* **295**, 334 (1966).

[43] W.H. Flygare, R.L. Shoemaker, and W. Huttner, *J. Chem. Phys.* **50**, 2414 (1969).

[44] S.L. Hartford, W.C. Allen, C.L. Norris, E.F. Pearson, and W.H. Flygare, *Chem. Phys. Lett.* **18**, 153 (1973)

[45] F.H.A. Rummens and S. Rajan, *J. Magn. Reson.* **31**, 497 (1978).

[46] F.J. Adrian, *Phys. Rev. A* **136**, 980 (1964).

[47] C.J. Jameson, *J. Chem. Phys.* **63**, 5296 (1975).

[48] F.H.A. Rummens and H.J. Bernstein, *J. Chem. Phys.* **34**, 2971 (1965).

[49] F.H.A. Rummens, W.T. Raynes, and H.J. Bernstein, *J. Phys. Chem.* **72**, 2111 (1968)

[50] L. Petrakis and H.J. Bernstein, *J. Chem. Phys.* **38**, 1562 (1963).

[51] J.A. Barker, R.O. Watts, J.K. Lee, T.P. Schaefer, and Y.T. Lee, *J. Chem. Phys.* **61**, 3081 (1974).

[52] G. Malli and C. Froese, *Int. J. Quantum Chem.*, **1S**, 95 (1967).

[53] D.K. Hinderman and C.D. Cornwell, *J. Chem. Phys.* **48**, 4148 (1968).

[54] N.F. Ramsey, *Phys. Rev.* **87**, 1075 (1952).

[55] C.J. Jameson, A.K. Jameson, and S.M. Cohen, *J. Magn. Reson.* **19**, 385 (1975).

[56] W.T. Raynes and B.P. Chadburn, *J. Magn. Reson.* **10**, 218 (1973).

[57] W.T. Raynes and B.P. Chadburn, *Mol. Phys.* **24**, 853 (1972).

[58] A.K. Jameson, K. Schuett, C.J. Jameson, S.M. Cohen, and H. Parker, *J. Chem. Phys.* **67**, 2821 (1977).

[59] C.J. Jameson, A.K. Jameson, and S.M. Cohen, *J. Chem. Phys.* **67**, 2771 (1977).

[60] R.A. Meinzer, Ph.D. Thesis, University of Illinois, 1965.

[61] A.K. Jameson, J.W. Moyer, and C.J. Jameson, *J. Chem. Phys.* **68**, 2873 (1978).

[62] C.J. Jameson, A.K. Jameson, and H. Parker, *J. Chem. Phys.* **68**, 2868 (1978).

[63] C.J. Jameson, A.K. Jameson, and H. Parker, *J. Chem. Phys.* **69**, 1318 (1978).

[64] C.J. Jameson and A.K. Jameson, *J. Chem. Phys.* **69**, 1655 (1978).

[65] C.J. Jameson, A.K. Jameson, and S. Wille, *J. Chem. Phys.* **83**, 3372 (1979).

[66] M. Toyama, T. Oka, and Y. Morino, *J. Mol. Spectrosc.* **13**, 193 (1964).

[67] H.H. Nielsen, *Rev. Mod. Phys.* **23**, 90 (1951).

[68] C.J. Jameson, *J. Chem. Phys.* **66**, 4977 (1977).

[69] I. Suzuki, *Appl. Spectrosc. Rev.* **9**, 249 (1975).

[70] R.M. Stevens, and W.N. Lipscomb, *J. Chem. Phys.* **40**, 2238 (1964).

[71] R.M. Stevens and W.N. Lipscomb, *J. Chem. Phys.* **41**, 184 (1964).

[72] E.B. Wilson, J.C. Decius, and P.C. Cross, *Molecular Vibrations,* McGraw-Hill, New York, 1955.

[73] A.D. Buckingham, *J. Chem. Phys.* **36**, 3096 (1962).

[74] D.R. Herschbach and V.W. Laurie, *J. Chem. Phys.* **35**, 458 (1961).

[75] K. Kuchitsu and Y. Morino, *Bull. Chem. Soc. Jpn.* **38**, 814 (1965).

[76] Y. Morino, Y. Kikuchi, S. Saito, and E. Hirota, *J. Mol. Spectrosc.* **13**, 95 (1964).

[77] Y. Morino, *Pure Appl. Chem.* **18**, 323 (1969).

[78] C.J. Jameson, *J. Chem. Phys.* **67**, 2814 (1977).

[79] J. Overend, private communications.

[80] K. Kuchitsu and L.S. Bartell, *J. Chem. Phys.* **36**, 2460, 2470 (1962).

[81] A.R. Hoy, I.M. Mills, and G. Strey, *Mol. Phys.* **24**, 1265 (1972).

[82] K. Machida and J. Overend, *J. Chem. Phys.* **50**, 4429 (1969).

[83] R.G. Parr and J.E. Brown, *J. Chem. Phys.* **49**, 4849 (1968).

[84] A.C. Luntz, J.D. Swalen, and R.G. Brewer, *Chem. Phys. Lett.* **14**, 512 (1972).

[85] W.G. Golden, A.C. Jeannotte II, C.C. Blackburn, and J. Overend, *Spectrochim. Acta, Part A* **33**, 901 (1977).

[86] T.R. Faulkner, C. Marcott, A. Moscowitz, and J. Overend, *J. Am. Chem. Soc.* **99**, 8160 (1977).

[87] B.J. Krohn, W.C. Ermler, and C.W. Kern, *J. Chem. Phys.* **60**, 22 (1974).

[88] P. Pulay, W. Meyer, and J. E. Bogg, *J. Chem. Phys.* **68**, 5077 (1978).

[89] R.J. Bartlett, I. Shavitt, and G.D. Purvis, *J. Chem. Phys.* **71**, 281 (1979).

[90] V.W. Laurie and D.R. Herschbach, *J. Chem. Phys.* **37**, 1687 (1962).

[91] L.S. Bartell, S.K. Doun, and S.R. Goates, *J. Chem. Phys.* **70**, 4585 (1979).

[92] L.S. Bartell, *J. Chem. Phys.* **70**, 4581 (1979).

[93] R.M. Stevens and M. Karplus, *J. Chem. Phys.* **49**, 1094 (1968).

[94] E.A. Laws, R.M. Stevens, and W.N. Lipscomb, *J. Chem. Phys.* **54**, 4269 (1971).

[95] T.B. Garrett and D. Zeroka, *Int. J. Quantum Chem.* **6**, 663 (1972).

[96] W.T. Raynes, A.M. Davies, and D.B. Cook, *Mol. Phys.* **21**, 123 (1971).

[97] E. Ishiguro and S. Koide, *Phys. Rev.* **94**, 350 (1954).

[98] D. Zeroka, *J. Chem. Phys.* **59**, 3835 (1973).

[99] R.D. Amos, *Mol. Phys.* **35**, 1765 (1978).

[100] A. Saika and C.P. Slichter, *J. Chem. Phys.* **22**, 26 (1954).

[101] R.F.W. Bader and A.D. Bandrauk, *J. Chem. Phys.* **49**, 1666 (1968).

[102] J.H. Letcher and J.R. Van Wazer, in *Topics in Phosphorus Chemistry,* M. Grayson and E.J. Griffith, Eds., Interscience Publishers, New York, 1967, Vol. 5, pp. 75-226.

[103] R.A. Bernheim and H. Batiz-Hernandez, *J. Chem Phys.* **45**, 2261 (1966).

[104] S.G. Kukolich and S.C. Wofsy, *J. Chem. Phys.* **52**, 5477 (1971).

[105] H. Batiz-Hernandez and R.A. Bernheim, *Prog. Nucl. Magn. Reson. Spectrosc.* **3**, 63 (1967).

[106] M. Cohn and A. Hu, *Proc. Natl. Acad. Sci. U.S.A.* **75**, 200 (1978).

[107] M. Cohn and B.D.N. Rao, *Bull. Magn. Reson.* **1**, 38 (1979).

[108] M.R. Bendall and D.M. Doddrell, *Aust. J. Chem.* **31**, 1141 (1978).

[109] M. Alei and W.E. Wageman, *J. Chem. Phys.* **68**, 783 (1978).

[110] W.M. Litchman, M. Alei, and A.E. Florin, *J. Chem. Phys.* **50**, 1897 (1969).

[111] A.K. Jameson and C.J. Jameson, *J. Magn. Reson.* **32**, 455 (1978).

[112] A.D. Buckingham and W. Urland, *Chem. Rev.* **75**, 113 (1975).

[113] C.J. Jameson, *J. Chem. Phys.* **66**, 4983 (1977).

[114] R.K. Harris and B.E. Mann, Eds., *NMR and the Periodic Table,* Academic Press, New York, 1979.

[115] C.J. Jameson and H.S. Gutowsky, *J. Chem. Phys.* **40**, 1714 (1964).

[116] P.C. Lauterbur, *J. Chem. Phys.* **42**, 799 (1965).

[117] H.J. Bernstein and A.D.E. Pullin, *J. Chem. Phys.* **21**, 2128 (1953).

[118] M. Wolfsberg, *Z. Naturforsch., Teil A* **18**, 216 (1963).

[119] A.A. Chalmers and D.C. McKean, *Spectrochim. Acta* **22**, 251 (1966).

[120] D.C. McKean, *Spectrochim. Acta* **22**, 269 (1966).

[121] J. Jokisaari, K. Raisanen, L. Lajunen, A. Passoja, and P. Pyykko, *J. Magn. Reson.* **31**, 121 (1978).

[122] J. Jokisaari and K. Raisanen, *Mol. Phys.* **36**, 113 (1978).

[123] C.J. Jameson and A.K. Jameson, *J. Chem. Phys.* **68**, 615 (1978).

[124] J.O. Hirschfelder, Ed., *Advances in Chemical Physics,* Wiley, New York, 1967, Vol. 12.

[125] D. Steele, in *Molecular Spectroscopy (Specialist Periodical Reports),* The Chemical Society, London, 1977, Vol. 5, p. 186.

[126] R.E. Hester, in *Raman Spectroscopy Theory and Practice,* H.A. Szymanski, Ed., Plenum Press, New York, 1967, p.101.

[127] G.E. Ewing, *Acc. Chem. Res.* **8**, 185 (1975).